U.S. DEPARTMENT OF THE INTERIOR

U. S. GEOLOGICAL SURVEY

GEOPHYSICAL INTERPRETATIONS WEST OF AND WITHIN THE NORTHWESTERN PART OF THE NEVADA TEST SITE

by

V. J. S. Grauch[1], David A. Sawyer[2], Chris J. Fridrich[2], and Mark R. Hudson[2]

Open-File Report 97-476

1997

[1]U. S. Geological Survey, MS 964, Federal Center, Denver CO 80225
[2]U. S. Geological Survey, MS 939, Federal Center, Denver CO 80225

GEOPHYSICAL INTERPRETATIONS WEST OF AND WITHIN THE NORTHWESTERN PART THE NEVADA TEST SITE

by
V. J. S. Grauch, David A. Sawyer, Chris J. Fridrich, and Mark R. Hudson

TABLE OF CONTENTS

FIGURES

FIGURES, CONTINUED

Page

TABLES

ABSTRACT

This report focuses on interpretation of gravity and new magnetic data west of the Nevada Test Site (NTS) and within the northwestern part of NTS. The interpretations integrate the gravity and magnetic data with other geophysical, geological, and rock-property data to put constraints on tectonic and magmatic features not exposed at the surface. West of NTS, where drill-hole information is absent, these geophysical data provide the best available information on the subsurface. Interpreted subsurface features include calderas, intrusions, basalt flows and volcanoes, Tertiary basins, structurally high pre-Tertiary rocks, and fault zones. New features revealed by this study include (1) a north-south buried tectonic fault east of Oasis Mountain, which we call the Hogback fault; (2) an east-striking fault or accommodation zone along the south side of Oasis Valley basin, which we call the Hot Springs fault; (3) a NNE-striking structural zone coinciding with the western margins of the caldera complexes; (4) regional magnetic highs that probably represent a thick sequence of Tertiary volcanic rocks; and (5) two probable buried calderas that may be related to the tuffs of Tolicha Peak and of Sleeping Butte, respectively.

INTRODUCTION

The study area (fig. 1) is located within the southwestern Nevada volcanic field (SWNVF), which has been the focus of extensive geologic, hydrologic, and geophysical investigations for more than thirty years. The studies were conducted in support of underground nuclear weapons testing at the Nevada Test Site (NTS) and nuclear waste storage activities at Yucca Mountain by the Department of Energy and its predecessor agencies. Recently, Laczniak and others (1996) used this extensive information to summarize the state of knowledge about ground-water systems in the NTS and Yucca Mountain region. Although they could draw on a vast data set of subsurface geologic information from hundreds of deep (>600 m) drill holes (Ferguson and others, 1994), these data are limited to local areas, especially in the vicinity of testing areas on the NTS. Thus, many important questions remain that are pivotal to understanding the pathways ground water will take outside the NTS (Laczniak and others, 1996). In particular, the deep ground-water systems west of the NTS are poorly understood. Better knowledge of this area is crucial for evaluating the possible pathways for ground water from testing areas at Pahute Mesa (fig. 1).

Because ground water flows at deep levels in this area, it is important to locate major subsurface features that have potential for controlling flow. In the absence of drill-hole information, geophysical maps provide one of the best ways to recognize major subsurface features. Moreover, where drill-hole information is present, geophysical data can provide an important tool for interpolating the geologic information between distant drill holes by defining geologic units expressed in the geophysical data. Therefore, in this report we rely heavily on geophysical data, especially gravity and magnetic data, to build a picture of major subsurface features in the study area. The interpretations are developed by integrating new aeromagnetic data, recent geologic mapping, and new rock-property measurements west of NTS with established gravity data and drill-hole information.

GEOPHYSICAL BACKGROUND

Geophysical studies of the NTS and vicinity have been conducted for decades concurrently with geologic and hydrologic studies. The geophysical methods that have been employed include gravity; ground-based and airborne magnetic, seismic reflection and refraction, teleseismic, heat flow, borehole geophysics, and a variety of deep-looking electrical methods, primarily the magnetotelluric method. However, gravity and magnetic data are the primary geophysical data sets available for the area west of NTS and north of Bare Mountain. In this report we focus on the gravity and magnetic data, integrated with geologic mapping and rock-property information.

Gravity Data

Data for over 19,000 gravity stations (fig. 2) were extracted from a data base described by McCafferty and Grauch (1997) and were interpolated onto a grid at 100 m intervals. McCafferty and Grauch compiled their data from Saltus (1988a) and Harris and others (1989). In order to isolate the gravity effects of the rocks in the upper crust, these authors removed a regional field from the Bouguer gravity values based on an isostatic model (Simpson and Jachens, 1989), described in Saltus (1988b). The same regional field was removed from the data for this study.

The typical value of 2670 kg/m^3 used to reduce gravity data is too large to be representative of subsurface densities for large areas of the SWNVF (Kane and others, 1981; Snyder and Carr, 1982). Measured rock densities of volcanic rocks in the SWNVF show extreme variability, ranging as widely as 1400 to 2500 kg/m^3 (Ferguson and others, 1994). Measurements within bore holes indicate that local density variations can be abrupt and unpredictable, depending on depth, structure, degree of welding, alteration (particularly zeolitization, which decreases density significantly), and water saturation (Healey, 1968; Snyder and Carr, 1982, 1984; Carroll, 1989; Ferguson and others, 1994). However, lithologies can be divided into several general groups of density ranges that are useful for looking at bulk density averages of the upper crust in the SWNVF (table 1). In figure 3, the isostatic residual gravity data is based on a reduction density of 2400 kg/m^3, which provides a compromise between the areas of high density surrounding the SWNVF versus areas of low density within the SWNVF.

Aeromagnetic Data

Interpretation of aeromagnetic data for the SWNVF is more difficult than for other geologic settings for several reasons. Remanent magnetization can be quite variable, ranging from low to high intensities, sometimes within the same unit. Thus, the total magnetization of the rocks is important to consider rather than just magnetic susceptibility or paleomagnetic direction (Bath, 1968; Grauch, 1987a). Total magnetization is the vector sum of the remanent and induced components, determined from paleomagnetic and magnetic-susceptibility measurements, respectively. Because the induced component by definition is aligned with the present-day Earth's field, total magnetization with a negative inclination must result from a strong reverse-polarity remanent component and produces characteristic, high-amplitude magnetic anomaly lows. Where this type of anomaly is recognized, one can develop the following conclusions about the source of the anomaly: (1) it is shallow (otherwise the

amplitude would be too low to recognize as a strong anomaly); and (2) it is probably an extrusive rock. The latter conclusion arises because strong remanent magnetization is usually carried by titanomagnetite of small grain size. Grains of the necessary size occur most frequently as the result of fast cooling or high-temperature oxidation (Larson and others, 1969), events expected primarily for extrusive rather than intrusive rocks.

In contrast to negative-inclination, a positive-inclination total magnetization can result from either a reverse- or normal-polarity remanent component. Units that have high magnetic susceptibilities and low remanent intensities and units that have high normal-polarity remanent intensities can both produce strong magnetic highs. Therefore, in this report we commonly refer to positive- or negative-inclination total magnetization rather than to normal- or reverse-polarity remanence. This acknowledges the ambiguity in interpreting magnetic highs without independent rock-property information.

In dealing with total magnetization, interpretation is simplified if one can assume that the total magnetization is collinear with the Earth's field. From examining rocks in the NTS, Bath (1968) developed the criterion that the remanent and induced components are considered collinear when they are within 25^{o} of each other. Thus, a wide range of total magnetization directions can be considered collinear. In practice we found that volcanic units that do not have collinear total magnetization directions in this area do not produce significant magnetic anomalies at the scale of study anyway. These units usually have low magnetic susceptibilities, and therefore negligible components in the direction of the total field. Relative total magnetizations of selected volcanic units for the study area are presented in table 2.

Another consideration for magnetic interpretation in the SWNVF is the presence of rugged topography composed of magnetic rocks. Magnetic methods in areas of rugged topography can use relations between anomaly shapes and topographic shapes to determine whether the source of the anomaly composes the topography or lies at depth (Grauch, 1987b). Positive correlation with topography indicates that rocks composing the topography have positive-inclination total magnetization; inverse correlation indicates negative-inclination total magnetization. Lack of correlation with topography or with mapped extent of geologic units suggests that the magnetic source underlies the units exposed at the surface. In addition, if it can be determined from the character of the magnetic anomaly that the buried source is an extrusive unit, the age of the overlying unit may place important constraints on the likely identification of the underlying source. Thus, understanding the relation of magnetic anomalies to exposed and buried rock units in the SWNVF is best accomplished by inspection of magnetic anomalies compared to topographic shapes, extent of mapped units, and using input from rock-magnetic property measurements.

Aeromagnetic data for this study were extracted from the compilation prepared by McCafferty and Grauch (1997), who merged fourteen individual surveys onto a common observation altitude of 122 m above ground. Most of the study area for this paper is covered by two detailed surveys (fig. 4), both flown at 122 m above ground with east-west flight lines spaced 400 m apart (Kane and others, 1981; Grauch and others, 1993). The west Pahute Mesa survey (Grauch and others, 1993) was recently acquired; interpretations from the new survey are introduced in this report. Due to weather-related problems, the survey was flown in two

segments, one spanning November 13-22, 1992, and the other April 24-28, 1993 (fig. 4). A lower resolution survey covers the area bounded from 36°45' to 37° latitude and 116°37.5' to 116°45' longitude (fig. 4). It was originally flown at 300 m above ground with north-south flight lines spaced 800 m apart (Langenheim and others, 1991), but was analytically continued to match the lower observation surface of the final compilation (McCafferty and Grauch, 1997).

Given the assumption of collinearity between total magnetization and the Earth's field vectors, the magnetic data were transformed by reduction-to-the-pole (fig. 5) in order to place anomalies directly over their sources (Blakely, 1995). Inclination and declination of the Earth's field used in the transformation were 62° and 14.5°, respectively. The reduction-to-pole transformation relocated many anomalies so that they directly correspond to mapped geologic units, allowing for confidence in the assumption of collinearity.

REGIONAL FEATURES

To a first order, the gravity map (fig. 3) shows fundamental differences in bulk density of the upper crust that are related to structural relief on the pre-Tertiary basement. The high values show where dense, pre-Tertiary rocks are near the surface; the low values show where these rocks are at great depths. Estimates of depths to the pre-Tertiary rocks using the iterative modeling method of Jachens and Moring (1990; Jachens and others, 1996) indicate that the pre-Tertiary rocks are generally 1 km below the surface where gravity values are positive (fig. 3; V. Langenheim, written commun., 1997). Where gravity values are less than about -10 mgals, depths to pre-Tertiary basement range from 2 to 8 km (V. Langenheim, written commun., 1997), indicating great thicknesses of low-density rocks (table 1). Gravity patterns within the Timber Mountain and Silent Canyon caldera complexes tend to be circular, a common characteristic of gravity anomalies associated with calderas (Plouff and Pakiser, 1972).

Depth estimates over gravity highs in the northern part of the area and in the northern Bullfrog Hills (1 and BH, fig. 6), indicate that pre-Tertiary rocks are less than 500 m below the surface (V. Langenheim, written communication). Corroborating evidence in the northern Bullfrog Hills are exposures of Paleozoic rocks in a local uplift and evidence of thin Tertiary section (C. Fridrich, unpub. mapping). A depth estimate from magnetotelluric data (Furgerson, 1982) shows a depth of about 1 km to resistive bedrock at the northeastern end of Springdale Mountain (fig. 1). In the northern part of the area, Paleozoic rocks are exposed near the western margin of the Black Mountain caldera (Sawyer and others, 1995). However, variations in the positive gravity values (fig. 3) may also be due to density variations within the pre-Tertiary rocks (table 1).

On the extreme west side of the study area is Sarcobatus Flat (fig. 1). The low gravity values (fig. 3; SF, fig. 6) indicate this is a deep basin. Regional estimates of the basin depth give about 1.5 to 2.0 km (Jachens and Moring, 1990; Jachens and others, 1996; Saltus and Jachens, 1995). The strong, broad, low magnetic anomaly (fig. 5) indicates a down-dropped block of volcanic rock having negative-inclination magnetization.

Regional variations in the magnetic map (fig. 5) are harder to see than in the gravity map because the magnetic data are sensitive to shallow sources. In order to see more regional

variations, we computed the magnetic potential of the data (fig. 7). The magnetic potential is an integration of the data (often called pseudogravity: Baranov, 1957; Blakely, 1995), which subdues the local variations and emphasizes the broad variations in the data. The map has been further filtered by the terracing method of Cordell and McCafferty (1989) in order to bring out discrete areas that have nearly the same values, analogous to a terraced hillside.

The values on the magnetic potential map (fig. 7) can be viewed as an indicator of the relative bulk magnetization of the subsurface. Exceptions occur where low magnetic-potential values were derived from strong negative anomalies that have wide lateral extent, such as features 9, 11, and 12 on the eastern side and feature 2 on the western side of the study area (figs. 5 and 6). Bulk magnetization can be high due to thick piles of rocks having moderate remanent magnetization (such as welded ash-flow tuffs or some basalts), moderate magnetic susceptibility (such as intermediate- to mafic-composition intrusions or lava), or both. At great depth, however, remanent magnetization is likely subdued due to thermal destruction (McElhinny, 1973). Thus, high bulk magnetization may imply the presence of large volumes of igneous rocks of intermediate composition. If so, the region of generally high bulk magnetization could show the general location of the deep intrusive roots to the volcanic field, or alternatively, of buried, intermediate-composition volcanic rocks.

INTERPRETED FEATURES

Major, interpreted geophysical features are labeled on figure 6. The exact locations of the outlines were guided primarily by the maximum horizontal gradients of the magnetic-potential or gravity data, which indicate the surface contacts of near-vertical boundaries (Cordell, 1979; Cordell and Grauch, 1985; Blakely and Simpson, 1986). These locations can be offset downdip if the boundaries have shallower dip (Grauch and Cordell, 1987).

Although the resulting maps reveal many interesting features, we limit our discussions to major features that cover fairly large areas or have significant linear extent. For example, many minor faults can be interpreted from magnetic data in the southern Bullfrog Hills (north of BA, fig. 5, 6), which is an area of tilted fault blocks. The striped pattern of north-trending magnetic anomalies evident in this area is similar to the pattern in Crater Flat and Yucca Mountain (north and west of CF, figs. 5 and 6; Bath and Jahren, 1984). Instead, only one major fault (4, fig. 6) interpreted from the magnetic data is shown on figure 6. This fault marks an abrupt change between north-south orientation (on the northwest) and northeast orientation (on the southeast) of the grain of tilted fault blocks (fig. 5). In addition, we have not included geophysical interpretations from the area around Yucca Mountain, because this area has been discussed extensively by other workers (e.g., Oliver and others, 1995).

Central Caldera Complexes

Calderas known from drilling or surface geologic mapping include the Area 20 and Grouse Canyon calderas (fig. 6, A20 and GC), comprising the Silent Canyon caldera complex (SCC, fig. 6); the nested Ammonia Tanks and Rainier Mesa calderas (ATT, ATS and RMT, RMS, respectively, fig. 6), comprising the Timber Mountain caldera complex (fig. 1); Black Mountain caldera (BM, fig. 6), and the Claim Canyon caldera (CC, fig. 6). The outlines for these

calderas are from Sawyer and others (1994, 1995), who based their locations on surface geologic contacts, thickness differences between caldera-forming and post-caldera units, and from scattered to tightly constrained subsurface drill-hole information (Warren and others, 1985; Ferguson and others, 1994). Ferguson and others (1994) interpret slightly different locations for parts of the caldera margins within the Silent Canyon caldera complex. The caldera margins are dashed on figure 6 where their locations are based on previous geophysical interpretations (Sawyer and others, 1994). In a modification to the margins of Sawyer and others (1994), we have not drawn the southwestern margin of the Rainier Mesa caldera on figure 6. This omission reflects a different outlook on the ambiguity of the geophysical information, discussed below.

The Grouse Canyon (13.7 Ma; GC, fig. 6) and Area 20 (13.25 Ma; A20, fig. 6) calderas of the Silent Canyon caldera complex are beneath Pahute Mesa (fig. 1). Both calderas are completely buried by younger deposits and were first identified by gravity studies (Healey, 1968; Orkild and others, 1968). Subsequently, more than a hundred deep (>600 m) drill holes have defined the subsurface distribution of volcanic units in the complex (Warren and others, 1985, Sawyer and Sargent, 1989; Ferguson and others, 1994; Sawyer and others, 1994). The eastern margin of the Grouse Canyon caldera and the northern topographic wall of the Silent Canyon caldera complex are reflected in abrupt changes in magnetic anomaly patterns (fig. 5).

The oldest caldera of the Timber Mountain caldera complex, the Rainier Mesa caldera, formed in response to the eruption of the Rainier Mesa Tuff (Tmr, table 2) at 11.6 Ma. The topographic wall of the caldera (RMT, fig. 6) is not tightly constrained geologically except along the northeastern margin. The topographic wall of the younger Ammonia Tanks caldera (11.45 Ma), is probably superimposed on the structural wall of the Rainier Mesa caldera along the southeastern margin (RMS/ATT, fig. 6). A portion of the resurgent, intracaldera dome of the Rainier Mesa caldera is exposed on the west side of the Ammonia Tanks caldera (near ATT western boundary), but the largest part of the caldera was stoped by the Ammonia Tanks caldera or is covered by younger rocks (Sawyer and others, 1994)

The structural and topographic margins of the Ammonia Tanks caldera (ATS, and ATT, respectively, fig. 6) are well exposed around most of the caldera. It is a classic resurgent caldera (Christiansen and others, 1977) of the type described by Smith and Bailey (1968), with isolated exposures of intrusive rocks related to resurgence located on the southeast side of Timber Mountain (Byers and others, 1976a, b). The geologic evidence, combined with analysis of the gravity data, led Kane and others (1981) to conclude that the broad, low-amplitude gravity high in this area is the expression of the resurgent intrusion (TM, fig. 6). Electrical-data profiles collected over Timber Mountain also indicated rocks with high resistivities at depth, typical of intrusive rock (Zablocki, 1979). The outline for this inferred resurgent intrusion on figure 6 was drawn at about the gravity contour level of -10 mgal (TM, fig. 6) for two reasons: (1) the gradients surrounding the gravity high are moderate, especially to the north, indicating the intrusive contacts gently slope downward and have no identifiable vertical "edges", and (2) inside this lateral extent, thickness estimates of caldera fill are less than 1 km (V. Langenheim, written commun., 1997), which are the most important depths to consider in relation to ground-water depths in the surrounding area (Lazcniak and others, 1996).

The Claim Canyon caldera (Byers and others, 1976a; Christiansen and others, 1977; Sawyer and others, 1994; Fridrich, in press) collapsed at 12.7 Ma, accompanied by the eruption of the Tiva Canyon Tuff (Tpc, table 2). Part of the intracaldera dome is exposed south of Timber Mountain (CC, fig. 6), but most of the caldera is beneath the younger Timber Mountain caldera complex. Gravity values within the exposed part of the caldera (CC, fig. 6) are higher compared to surrounding areas (fig. 3), suggesting the presence of a resurgent intrusion, analogous to the one under Timber Mountain. The caldera margins correspond to an abrupt change in magnetic-anomaly pattern (fig. 5).

The topographic margin of the youngest caldera, the Black Mountain caldera (9.4 Ma; BM fig. 6), is a contact with precaldera rocks, well-exposed for more than half its boundary. Within the caldera is a thick (at least 500 m) sequence of the mafic Trachyte of Hidden Cliff (Tth, Table 2), which extruded as a dome within the caldera depression (Sawyer and others, 1995). This unit produces strong positive magnetic anomalies where it is exposed (fig. 5; fig. 8). The great thickness of this magnetic unit is also expressed as high magnetic values on the magnetic potential map (fig. 7). The unit is surrounded by a negative-anomaly-producing unit(s), most likely the trachytic rocks of Pillar Spring and Yellow Cleft (Tts, Table 2; fig. 8). In addition, a circular gravity high corresponds fairly well to the caldera outline (fig. 3). A simple profile model across the high (A-A', fig. 6) shows that the anomaly cannot be explained solely by high-density mafic extrusive rocks (fig. 9a). The lateral extent of the extrusive rocks, which is determined by the location of the topographic wall of the caldera, does not extend far enough on either side of the profile to account for the broad anomaly. Therefore, a buried dense source must also be present. A simple model of an intrusion (fig. 9b) demonstrates that a moderate-density intrusion can explain the breadth of the gravity high.

Possible Buried Tolicha Peak(?) Caldera

The western topographic wall of the Black Mountain caldera crosses a very strong magnetic positive anomaly that has an east-west elongated negative anomaly to the north and northwest (fig. 8). The boundary between the two anomalies is a sharp, linear east-west gradient, which has the same orientation as mapped faults in the area (Sawyer and others, 1995). Other than this indirect correspondence, the anomaly has no relation to mapped geology nor to topography (fig. 8). This lack of correspondence, the very large amplitude, steep gradients, and the lack of associated gravity highs (fig. 3), suggest the source of the positive anomaly has high remanent magnetization and shallow depth extent. These observations can be explained by an extrusive rock unit that underlies and is older than the surface geologic units, and therefore is older than the fill of the Black Mountain caldera. This explanation requires that the western topographic wall of the Black Mountain caldera has a shallow slope overlying the source of the positive anomaly; that is, the caldera fill has no magnetic expression here because it is thin.

The oldest unit mapped in the area of the positive anomaly is the middle rhyolite of Quartz Mountain (Tqh, table 2), which does not have sufficiently high magnetization nor spatial correspondence to the high to be the source. An older unit with the required magnetization is the strongly magnetic tuff of Tolicha Peak (Tqt, Table 2). Nearby, the tuff of Tolicha Peak is exposed and produces similar, strong magnetic highs (fig. 8).

The most likely explanation for the negative anomaly is an extrusive unit having a negative-inclination magnetization, because of the strong amplitude of the anomaly and steep gradients on its sides (fig. 8). In addition, the unit must be older than and underlie the volcanic units exposed at the surface due to the lack of correspondence to geology and topography. The oldest unit mapped in the area of the negative anomaly is early rhyolite of Quartz Mountain (Tqe, table 2; Sawyer and others, 1995), which is only weakly magnetic. Thus, the negative anomaly is produced by a volcanic unit that is older than any of the volcanics of Quartz Mountain (Tq, table 2), and cannot be identified as any other older unit mapped in this area (fig. 8, table 2; Sawyer and others, 1995).

The juxtaposition of the positive anomaly, interpreted to represent tuff of Tolicha Peak (Tqt, table 2), and the negative anomaly, interpreted to represent a pre-Tolicha Peak volcanic unit, at a steep linear gradient (fig. 8) can be explained by a caldera margin. Several other lines of evidence, when considered collectively, add weight to the suggestion that the linear gradient represents the northern margin of a caldera and probable source of the tuff of Tolicha Peak. First, the circular extension of low gravity values just to the south of this area (5, fig. 6; fig. 3) has a caldera-like shape, and indicates an area filled with a thick sequence of low-density rocks. The size of this circular area is commensurate with the expected size of the caldera from which the tuff of Tolicha Peak was erupted. Second, although there is no surface evidence of a caldera margin near the western side of this circular gravity low, the Rainier Mesa and Grouse Canyon Tuffs (Tmr and Tbg, table 2; fig. 14) are thin near this margin and appear to have lapped up around the edge of a circular, paleo-topographic high when they were deposited (Sawyer and others, 1995; S. Minor, oral commun., 1996). On the basis of additional geologic evidence, Christiansen and others (1977) also argued that this area (5, fig. 6) was the source of the tuff of Tolicha Peak, but called it the Sleeping Butte caldera. Finally, the mapped tuff at Tolicha Peak (fig. 8) is thick (> 300 m) and thickens generally southward (S. Minor, USGS, oral commun., 1996). Although the geophysical evidence suggests the presence of a caldera, evidence that questions its source as the tuff of Tolicha Peak is caldera-collapse breccia observed within the tuff on Tolicha Peak (fig. 1), 5 km away (C. Fridrich, unpub. mapping). The discrepancy in location of the proposed caldera and this breccia, which indicates an intracaldera setting or close proximity to the Tolicha Peak caldera, can be explained by transport during later structural modification. However, evidence of such transport has not been recognized. Alternatively, the geophysical data represent an unidentified, buried caldera.

Possible Buried Sleeping Butte(?) Caldera

A prominent, elliptical gravity low in the northwestern part of the study area (3, fig. 6; fig. 3) is likely a buried caldera, and possibly the source of the tuff of Sleeping Butte (Tqs, table 2). The gravity low is located in an area with very few bedrock exposures (fig. 10), and its outline corresponds in places with discontinuities or abrupt changes in character in the magnetic map (fig. 5). Depth estimates to the top of magnetic rocks within the area of the low using a match-filtering technique (program MFILT in Phillips and Grauch, in press) indicate the volcanic rocks are buried by an average 300-400 m of effectively nonmagnetic (probably alluvial) material. The gravity low was inverted using a simple three-dimensional basin model (Cordell and Henderson, 1968) and assuming predominantly volcanic fill with a density contrast of -320 kg/m^3 (which fits a presumed density of 2670 kg/m^3 for pre-Tertiary rocks and 2350 kg/m^3 for

the fill). The model indicates a broad, gentle depression within the pre-Tertiary rocks that has maximum depth of 1.9 km. Depths to the bottom of the depression would proportionally increase or decrease assuming, respectively, a greater or lesser density contrast.

In the area of the gravity low, the volcanic units within the fill cannot be identified definitely, but several constraints can be placed on their possible identification from the magnetic anomalies. First, in order to better view the magnetic anomalies, the magnetic data were analytically continued down only in the area of the gravity low. The continuation enhances details of the anomalies and allows better comparison with anomalies outside the area of the low. The procedure simulates how the magnetic data would have been observed had the section of alluvium been stripped away and the survey plane allowed to fly at constant clearance above the volcanic rocks. The data were continued downward to a surface (Cordell, 1985) that smoothly descends to a maximum depth of 500 m in the middle of the gravity low, giving depths to volcanic rocks that average close to the estimates given by MFILT. The smoothness of the continuation surface was chosen to avoid discontinuities that would cause instabilities in the downward-continution operation. In addition, lowpass filtering was applied to reduce problems related to continuation of circular anomalies produced by sources that extend above the continuation surface, discussed next.

The resulting, continued magnetic map (fig. 10) enhances a number of small circular magnetic highs within the eastern portion of the area of the gravity low. In the middle of the gravity low, the magnetic highs correspond to exposed rhyolite domes, currently mapped as middle rhyolite of Quartz Mountain (Tqh, table 2; Sawyer and others, 1995). However, the field relations are somewhat uncertain and the domes may be younger than the tuff of Sleeping Butte (S. Minor, USGS and R. G. Warren, Los Alamos National Laboratory, oral comm., 1996). Moreover, the rhyolite of Quartz Mountain would not be expected to produce positive anomalies (table 2). Whatever their age, the presence of rhyolite domes is suggestive of post-caldera volcanic activity within a caldera or caldera moat.

The sources of other magnetic anomalies in the area do not seem to be related to the inferred depression. The strong, semi-linear negative magnetic anomaly at Coba Ridge just to the southwest of the area of the gravity low (CR, fig. 6) corresponds well to the mapped extent of younger Tertiary basalt (fig. 10) that has a strong, negative-inclination total magnetization (Tyb, table 2). This unit is younger than basalt mapped as the same unit directly to the north (fig. 10), which has normal-polarity remanent magnetization (M. Hudson, unpub. data) and upon which the Gold Flat tuff was deposited (labeled as Tv on fig. 10). The older basalt overlaps the area of strong negative magnetic anomaly on the western side of the area of the gravity low (2, fig. 6; fig. 10). Therefore, because (1) the high-amplitude of the negative anomaly is typical of an extrusive unit, and (2) negative magnetic anomalies are not expected from the older basalt, the source producing this anomaly must be an extrusive unit that underlies and thus is older than the older basalt. A likely candidate is the Rainier Mesa Tuff (Tmr, Table 2), which is exposed nearby and corresponds to lower amplitude negative anomalies just outside the western edge of the area of the gravity low (fig. 10). The presence of Rainier Mesa Tuff in the subsurface is also likely southeast of Coba Ridge, where a knob of Ammonia Tanks Tuff, expected to produce positive anomalies (Tma, table 2), is located near the minimum of a high-amplitude negative anomaly (fig. 10).

Evidence that supports a caldera origin for the depression is (1) geological and geophysical evidence of rhyolite domes confined within the area of the gravity low, and (2) general thickening of the tuff of Sleeping Butte and the tuff of Tolicha Peak toward the area of the gravity low, (S. Minor, oral commun., 1996). If the depression represents a caldera, then it must pre-date the older basalt that underlies the Gold Flat Tuff, as discussed above.

Evidence that does not support, but does not necessarily preclude, a caldera origin are (1) the low bulk magnetization for the area (fig. 7), and (2) lack of definitive identification of a corresponding tuff unit. First, moderate to high bulk magnetization in the area is expected (but not required) by analogy to the area of main caldera formation (fig. 7), where moderate to high bulk magnetization is best explained by the presence of a large body of crystallized magma that originally fed the caldera eruptions. Intrusive rock of the same magnetic character would then also be expected in the area of the gravity low, if it represents a caldera of pre-Gold Flat Tuff age. Second, the magnetic character of the tuff of Sleeping Butte is not well determined (Tqs, Table 2), which does not allow confident comparison to the magnetic character within the area of the gravity low.

WNW-Striking Lineament

A west-northwest striking lineament (8, fig. 6) in the magnetic data (figs. 5 and 11) can be traced from the eastern side of the Black Mountain caldera (BM, fig. 6) to the eastern edge of the study area. The western part of the lineament is expressed as the boundary between strong negative anomalies on the northern side juxtaposed against higher magnetic values on the southern side. The central and eastern parts are expressed as linear positive anomalies, in places flanked on either side by strong negative anomalies. The extreme western and eastern parts are also expressed by subtle gravity gradients (Kane and others, 1981; not evident on fig. 3). From its linearity, a structural origin can be inferred. However, its genesis and age in relation to caldera formation are unknown.

Along the central part, the lineament coincides with the topographic wall of the Rainier Mesa caldera (RMT, fig. 6; fig. 11). Exposed north of the topographic wall are middle Paintbrush Group lavas and tuffs (Tpc, table 2; Tp, undifferentiated) that have reverse-polarity remanent magnetization (Sawyer and others, 1995). The magnetic anomalies are positive and high-amplitude, but have negative correlation with topography (hills produce lows; valleys produce highs). This negative correlation indicates that the rocks have strong, negative-inclination total magnetizations, as expected from the measured magnetizations (Table 2). The Paintbrush units in turn are overlain by the Rainier Mesa Tuff (Tmr, table 2), which also has strong negative-inclination total magnetization. This package of negative-anomaly producing rocks, with significant but variable thickness, are present in drill holes to the north (Ferguson and others, 1994) within the area of high-amplitude negative values (9, fig. 6; fig. 11), and likely explain the negative anomaly. Immediately south of the topographic wall are isolated exposures of the Ammonia Tanks Tuff (fig. 11). This tuff has strong, positive-inclination total magnetization (Tma, Table 2), and may explain some of the positive magnetic anomaly along the southern side of the lineament (fig. 11). Further south of the topographic wall, negative magnetic anomalies (10, fig. 6) correspond to moat lavas that have negative-inclination magnetization (Tmat, Table 2; fig. 11; Kane and others, 1981).

Along the eastern portion of the lineament, the topographic wall of the Rainier Mesa caldera is mapped to the north of the lineament (fig. 11). In this area, the lineament is defined as a linear positive magnetic anomaly that divides two high-amplitude negative anomalies (11 and 12, fig. 6). The northern negative anomaly (11) typifies an extrusive unit with negative-inclination total magnetization because of its high amplitude. However, it corresponds in location to the positive-anomaly-producing Ammonia Tanks Tuff (Tma, table 2; fig. 11), so the source of the negative anomaly likely underlies a thin layer of the Ammonia Tanks Tuff. A likely candidate is the Rainier Mesa Tuff (Tmr, table 2) which is exposed near the topographic wall (fig. 11). In addition, corresponding gravity values are greater than -10 mgal (fig. 3) and are more similar to gravity values over moderately deep pre-Tertiary rocks outside of the caldera areas than to the low gravity values representing deep pre-Tertiary rocks within the caldera complexes. One explanation is that this part of the topographic wall formed as a shallow scoop on top of pre-Tertiary rocks and the Rainier Mesa Tuff ponded within the shallow depression.

In contrast, the high-amplitude negative magnetic anomaly south of the lineament (12, fig. 6; fig. 11) is associated with low gravity values typical of caldera fill (fig. 3). Its magnetic signature also indicates an extrusive volcanic unit with strong negative-inclination magnetization (fig. 11). The Rainier Mesa Tuff (Tmr, Table 2) is likely the source, but the area is blanketed by younger, weakly magnetic rocks (fig. 11).

Along the western part of the lineament, magnetically insignificant Thirsty Canyon Group units (Tt, table 2) cover the surface (fig. 11). The positive magnetic values south of the lineament indicate rocks of moderate magnetization below the Thirsty Canyon Group (within about the top 1 km), such as the Ammonia Tanks Tuff, or Topopah Spring Tuff (Tpt, table 2). Where the positive anomalies are juxtaposed against the strong negative anomaly surrounding the two drill holes in the north-central part of figure 11, the anomaly amplitudes on both sides of the lineament are about the same (near 300 nT). The strength of the negative anomaly implies that the source rocks have strong negative total magnetization. In contrast, the low amplitudes of negative anomalies further to the west, along the northern side of the lineament, may represent a geometric effect caused by an abrupt termination of the moderately magnetized rocks on the south. Isopach maps from the drill holes in the area of the strong negative anomaly (fig. 11) indicate that the rhyolite of Benham (Tpu, table 2) has greater thickness there compared to other areas within the Silent Canyon Caldera complex (J. Wagoner, Lawrence Livermore National Laboratory, written commun., 1996). The drill hole on the south side at the western extreme of the lineament is not located within the Silent Canyon Caldera complex and therefore is not useful for comparison with the other two drill holes.

NNE-Striking Structures

The western margin of the Silent Canyon caldera complex (SCC, fig. 6) coincides with a NNE-trending gravity gradient (7, fig. 6; Sawyer and Sargent, 1989; Ferguson and others, 1994). The gravity gradient extends southwest of the complex and past the western side of the Timber Mountain caldera complex to Oasis Valley basin (fig. 1). Nearly parallel to and west of the gravity gradient is a magnetic gradient (6, fig. 6). The magnetic gradient is clearly expressed in the magnetic potential map as the edge of regional magnetic highs (RHN and RHS, fig. 7). The gradient appears as an irregular edge on the magnetic map (fig. 5), but its expression is more

linear on the magnetic potential map (fig. 7), indicating that the irregularities along the boundary in figure 5 are due to shallow sources. The coherency and linearity of both the magnetic and gravity gradients, and the abrupt changes in geophysical character across them (figs. 3, 5 and 7) indicate major structures at depth that juxtapose subsurface rocks having very different physical properties. Moreover, the direct relation between the gravity gradient and the Silent Canyon caldera margin (SCC and 7, fig. 6) is evidence that the gravity gradient reflects a structural zone here that is related to caldera formation. By extension then, the entire lengths of the magnetic and gravity gradients are probably related to each other and to caldera formation. The zone may have been a pre-existing structural zone that controlled the location of caldera margins during different periods of collapse.

The regional magnetic highs (RHN and RHS, fig. 7) bounded on the east by the NNE-striking structures correspond to moderately low gravity values (fig. 3). Rough depth estimates made from the gravity data, and corroborated by magnetic analysis, indicate that the source rocks of these regional magnetic highs extend at least 1 km below the surface. Another regional magnetic high (RHW, fig. 6) extends over the area of moderately high gravity values (fig. 3). Gravity inversion (V. Langenheim, written commun., 1997) indicates the thickness of Tertiary and younger rocks ranges from 500 m to 1 km. Arguments for which rock units are likely as sources for the regional magnetic highs at depth are discussed in the next sections.

Magnetic Sources Northeast of Black Mountain

Likely sources of the regional magnetic high northeast of Black Mountain (RHN, fig. 7) can be interpreted from the relation of magnetic anomalies to exposed rocks and from limited drill-hole information. Of the exposed units, a magnetic subunit (M. Hudson, unpub. data) of the comendite of Ribbon Cliff (Ttc, Table 2) locally contributes to the magnetic high near the margins of the Black Mountain caldera (figs. 8, 12). This is evident from the correlations between magnetic anomalies, topography, and mapped geologic units.

Likely primary contributors to the regional magnetic high were determined from limited drill hole information in the area (Ferguson and others, 1994). Drill hole PM-2, which was drilled to 2.7 km depth, is situated within the magnetic high (fig. 12). Drill holes Ue20p and Ue20j, which penetrated similar units, are both located within the area of lower magnetic values in between the NNE structural zone on the west and the Silent Canyon caldera complex margin on the east (fig. 12). Primary contributors are units from PM-2 that are magnetically significant (table 2), have sufficient thickness compared to their depths of burial to produce magnetic highs, and are not present or are too deep to produce magnetic anomalies in the other two drill holes. Units that meet these criteria are the tuff of Tolicha Peak and the dacite of Mount Helen (Tqt and Tqm, respectively, table 2). Conversely, the Rainier Mesa Tuff (Tmr, table 2), which produces high-amplitude negative anomalies, is absent in PM-2 and present in significant thickness near the surface in the other two drill holes.

The tuff of Tolicha Peak has generally strong positive-inclination total magnetization. Although the magnetization appears variable from measured rock samples, exposures of the tuff have a consistent correspondence to the strong magnetic highs west of Black Mountain near Tolicha Peak (fig. 8). Moreover, depth estimates from anomalies about 1 km north of PM-2

using the gradient method of Phillips (program HDEP in Phillips and Grauch, in press) give depths to the top of the magnetic sources as about 200-300 m, the level where the tuff of Tolicha Peak was encountered in PM-2 (appendix of Ferguson and others, 1994).

Lavas correlated with the dacite of Mount Helen (Tqm, table 2) were encountered in the bottom 1.5 km of PM-2 (appendix of Ferguson and others, 1994). Rock-magnetic-property measurements from the dacite of Mount Helen collected from one site near Mount Helen, about 15 km to the northwest of PM-2, give a strong, positive total magnetization, but with shallow inclination. However, the direction of magnetization may be affected by tilt (M. Hudson, unpub. data). Comparisons of magnetic anomalies to an isolated exposure of this unit located outside of the study area 6 km to the north of PM-2 (Sawyer and others, 1995) show that the unit has sufficient magnetization to produce significant magnetic highs (cf. Cornwall, 1972 and McCafferty and Grauch, 1997).

Units from the Timber Mountain group, including the significant negative-anomaly producer, the Rainier Mesa Tuff (Tmr, table 2), are absent from PM-2 and present in most other drill holes on Pahute Mesa (Ferguson and others, 1994). Geologic evidence also suggests that the Rainier Mesa Tuff thins or is absent in the area of the regional magnetic high, whereas it is fairly thick, near the surface, and widespread elsewhere in the study area (Sawyer and others, 1995; Ferguson and others, 1994). Thus, magnetic anomalies may be subdued or negative in most of the area where the Rainier Mesa Tuff is present.

A simple model (fig. 13) of a magnetic profile that crosses from the regional magnetic high into the Silent Canyon caldera complex (B-B', fig. 12) shows that three magnetically significant units (dacite lavas, Tuff of Tolicha Peak, and Rainier Mesa Tuff) account for most of the variations in the magnetic data. High-frequency magnetic variations not fit by the model can be explained by variations in thicknesses and magnetizations of shallow rocks. The configuration of the bodies attributed to the dacite lavas account for the first-order variations along the profile. This is especially evident by comparing the fit between observed values after upward continuation by 1 km compared to the model values computed at the same high level (fig. 13). The variations due to shallow, thin rock units are reduced considerably by upward continuation. Near the caldera margin, the model shows a thickening of the modeled Rainier Mesa Tuff (Tmr). Viable models require either thickening, changes in magnetization, or variations in other rock units in this area. However, for simplicity, the chosen model only shows the first possibility.

Magnetic Sources Beneath Thirsty Mountain

The sources of the regional magnetic high (RHS, fig. 7) south of Black Mountain and in vicinity of Thirsty Mountain are mostly buried by younger rocks (fig. 14) and cannot be determined definitively. However, most of the units mapped at the surface can be ruled out.Except for the comendite of Ribbon Cliff (Ttc, table 2), which correlates well with magnetic anomalies and topography around the southern edge of the Black Mountain caldera, the oldest exposed rocks in the area of the regional magnetic high do not have magnetic properties that could produce the high (fig. 14). These rocks include tuffs of the Thirsty Canyon Group (Ttt, Ttg, table 2) and basalts erupted from the Thirsty Mountain shield volcano (Typ, Table 2), which

have shallow-inclination and negative-inclination total magnetizations, respectively. Additional evidence that the Thirsty Canyon Group tuffs are not sources of the magnetic high is a lack of correspondence between variations in the magnetic high compared to topography, especially northeast of Thirsty Mountain where canyons have cut down-section, exposing different units. Various other Tertiary and Quaternary basalts (Tyb and Qby, Table 2; Fleck and others, 1996) are sufficiently extensive and do not have consistent correspondence to magnetic highs to be major contributors (fig. 14).

At Thirsty Mountain itself, short-wavelength negative anomalies corresponding to basalt erupted from the Thirsty Mountain shield volcano (Typ, table 2; fig. 14) are superimposed on the regional magnetic high (TH, fig. 6). Paleomagnetic samples collected from basalts over the entire surface of the shield volcano indicate that the basalts have reverse polarity and were erupted in a relatively short time (Fleck and others, 1996). The magnetic map, however, shows the strong negative anomalies in a limited area surrounding a small magnetic high corresponding to the mapped vent of the volcano (fig. 14). Near the limits of mapped basalt, the lower magnetic values generally correspond to broad topographic ridges. This relation suggests the basalt is thickest in these areas.

The strong negative anomaly about 4.5 km north of the Thirsty Mountain edifice (fig. 14) is due to an unknown source. It is likely an extrusive rock, because it must have strong remanent magnetization with reverse polarity. In addition, it must be older than the basalt of Thirsty Mountain because it is buried below older units within the Thirsty Canyon Group (table 2).

Within the area of the regional magnetic high (RHS, fig. 7), the gradient method gives estimates of 250-300 m to the top of the sources of the regional magnetic high and indicates a large depth extent (greater than 500 m). Low-density volcanic rocks in this area are about 5 km thick (V. Langenheim, written commun., 1997). By analogy with the interpretation of the regional magnetic high to the north (RHN, fig. 7), lavas correlative to the dacite of Mount Helen or other intermediate-composition igneous rocks may be present at depth. Other likely contributors to the regional high can be determined from units that produce large-amplitude positive magnetic anomalies in the surrounding area. These include (from oldest to youngest, table 2) the tuff of Tolicha Peak (Tqt), the tuff of Sleeping Butte (Tqs), Ammonia Tanks Tuff (Tma), the rhyolite of Fleur-de-lis Ranch (Tff), and the comendite of Ribbon Cliff (Ttc; northern part of RHS only). Although the tuff of Sleeping Butte does not produce magnetic anomalies on the western side of Sleeping Butte, it is quite magnetic where it was sampled on the eastern side (fig. 14; Tqs, table 2). In addition, by analogy to the northern high (RHN, fig. 7), the general lack of subdued magnetic values (away from Thirsty Mountain basalt, TH, fig. 6) suggest that the Rainier Mesa Tuff (Tmr) is absent. However, an equally plausible explanation, in the absence of drill-hole information, is that Rainier Mesa Tuff is covered by a significant thickness of younger rocks having strong positive-inclination total magnetization, such as Ammonia Tanks Tuff (Tma) or the rhyolite of Fleur-de-lis Ranch (Tff, table 2; fig. 14).

Magnetic Sources North of Oasis Mountain

The regional magnetic high (RHW, fig. 7) north of Oasis Mountain (fig. 1) corresponds to moderate gravity values. Estimates from the gravity data indicate that the depth to pre-Tertiary rocks in the area ranges from 500 to 1000 m, whereas similar depth estimates to pre-Tertiary rocks in the areas of the adjacent regional magnetic highs (RHN and RHS) are about 5 km (V. Lanmgenheim, written commun., 1997). Bedrock is exposed within the western magnetic high (RHW) west of Thirsty Mountain (fig. 14) and is exposed to the southwest of the magnetic high at Springdale Mountain (figs. 1 and 14). However, Quaternary alluvium coincides with most of the magnetic high between these areas (fig. 14). Depth estimates using the gradient method place the tops of the magnetic sources within the area of alluvial cover to be about 100 m below the surface, with thicknesses exceeding 400 to 700 m, deepening to the north.

Two observations suggest that most of the buried magnetic rocks are probably tuff of Tolicha Peak (Tqt, table 2), which produces strong positive anomalies to the north (fig. 8). First, about 4 km south of Sleeping Butte, exposures of the tuff are associated with a strong magnetic anomaly that aligns with anomaly trends within the area of alluvial cover (fig. 14). Second, the structural grain of the buried magnetic sources trends northeast (fig. 14), a trend that is corroborated by magnetotelluric data near Springdale Mountain (Klein, 1995). The northeast trends are characteristic of structural events of an age that affected only rocks older than the volcanics of Fortymile Canyon (Hudson and others, 1996; table 2), suggesting that the magnetic sources are older than these units.

Magnetic Sources Northwest of Timber Mountain

A regional magnetic high from the magnetic potential map (RHE, fig. 7) is contained within the inferred topographic wall of the Ammonia Tanks caldera (ATT? on fig. 6) but extends outside the resurgent dome. It does not have a corresponding expression in the gravity data. The positive-anomaly-producing Ammonia Tanks Tuff (Tma, table 2) is exposed in the area, and depth estimates using the gradient method indicate that the magnetic source extends greater than 500 m in depth. Therefore, the primary source of the magnetic high is probably the Ammonia Tanks Tuff. The high magnetic values compared to surrounding areas within the Ammonia Tanks caldera (fig. 5) indicate that the Tuff is thicker or more magnetic here, or that younger rocks with negative-inclination magnetization (such as Tmat, Table 2) are not present, or both.

Oasis Valley Basin

The large area (14, fig. 6) east of Oasis Mountain and west of Ammonia Tanks caldera is an area of low gravity values (fig. 3), reflecting a thick sequence of moderately low-density rocks, probably Tertiary in age. The area is covered by alluvium with only a few bedrock exposures (fig. 15), and has very little magnetic signature (fig. 5). Depth-estimates from gravity data give a 5 km thickness of low-density rocks within the area (V. Langenheim, written commun., 1997). Drill hole Coffer #1, drilled for purposes of oil exploration, shows that the thickness of alluvium in the middle of this area is about 240 m (fig. 15a). The alluvium rests on Thirsty Canyon Group and older volcanic units, many of which are exposed at the surface nearby (fig. 15). We call this area of low gravity values "Oasis Valley basin" to clarify its location and

geologic significance (fig. 1). "Oasis Valley" is generally restricted on topographic maps to refer to the area labeled as "Oasis Valley discharge area" on Figure 1, but has sometimes been informally applied to a more extensive area, causing confusion.

The basin is bounded on the west by a major, inferred, north-striking fault mainly evident as a major gravity gradient (13, fig. 6), which we call the Hogback fault; on the south by an east-striking inferred structure evident in both magnetic and gravity maps (15, fig. 6), which we call the Hot Springs fault; and on the north by the abrupt, southern edge of a regional magnetic high (RHS, fig. 7; fig. 15). The eastern boundary and the origin of the thick sequence of low-density rocks beneath the basin are unclear. The thick sequence could represent either caldera fill or basin fill, probably of Tertiary age in either case. It represents caldera fill if one or more of the component calderas of the Timber Mountain complex (either the Rainier Mesa caldera, or an older buried caldera) utilized part of the Hogback fault (13, fig. 6) during caldera collapse. The caldera(s) would then extend from the exposed Timber Mountain caldera complex westward to the fault. (The lack of low gravity values to the west of the fault and the uninterrupted extent of the gravity gradient do not support the presence of a major caldera collapse west of the fault.) Alternatively, if a caldera does not extend as far west as the Hogback fault, the thick sequence of low-density rocks represents basin fill (either volcanic or sedimentary), which would have been deposited during tectonic subsidence. There is not enough geologic or geophysical evidence to establish which is the case.

The linearity of the north-striking gravity gradient associated with the Hogback fault (13, fig. 6) suggests a tectonic origin. The slope of this gravity gradient indicates a boundary dipping about 45°, which may represent one or a series of normal faults down to the east. This configuration is similar to the stepped-fault model of the Bare Mountain fault (16, fig. 6; Snyder and Carr, 1984; Carr, 1988, Oliver and Fox, 1993; Langenheim, in press). The northern extent of the inferred fault, where it passes along the west side of the area of Thirsty Mountain basalts (TH, fig. 6), is parallel to mapped faults (Minor and others, 1996) and nearly coincides with an east-facing paleoscarp (fig. 14a), where Ammonia Tanks Tuff was emplaced against volcanics of Quartz Mountain (Noble and others, 1991; Sawyer and others, 1995). Previous workers have interpreted this paleoscarp as evidence for a caldera topographic wall, although they disagree on the age of the caldera (Byers and others, 1976a; Noble and others, 1991). The paleoscarp may be surface evidence of the inferred tectonic fault or of caldera collapse that was controlled by the fault.

The steepness of the gravity gradient along the eastern half of the Hot Springs fault or transverse zone (15, fig. 6; fig. 3) indicates a near-vertical boundary; its linearity suggests a tectonic origin. It is also expressed by an abrupt change in magnetic character (fig. 5). Geologic evidence south of the fault indicates a paleoscarp there, with a depositional basin to the north during and perhaps before the time of deposition of the Rainier Mesa Tuff (C. Fridrich, unpub. data). However, field relations cannot clearly determine whether the structure is a caldera margin or the eroded scarp of a tectonic fault. The western half of the fault is expressed by an abrupt change in magnetic character and by a gravity gradient opposite in slope to the gradient along the eastern half of the fault (15, fig. 6; figs. 3 and 5). The juxtaposition of seemingly different gravity sources along the abrupt, linear juxtaposition of different magnetic patterns is consistent with the interpretation of a transverse structure along the Hot Springs fault.

Bare Mountain Area

Gravity highs are associated with uplifted and exposed Precambrian and Paleozoic rocks in Bare Mountain and the Funeral Mountains (BA, FU, fig. 6; fig. 3). The intervening Amargosa Valley (AV, fig. 6) is associated with moderate gravity values (fig. 3). The moderate gravity values suggest that the valley is fairly shallow and is floored by pre-Mesozoic rocks similar to those exposed nearby (Snyder and Carr, 1982, 1984; Carr, 1990). However, magnetotelluric data indicate that the crust below the valley fill has a somewhat different electrical character compared to the surrounding mountains; it is more resistive to much greater depths (Klein, 1995).

The general lack of magnetic anomalies within the Amargosa Valley in the study area indicates a corresponding lack of volcanic units (Kane and Bracken, 1983; Snyder and Carr 1982, 1984). An exception is a broad magnetic high near the Funeral Mountains (17, fig. 6). The high is associated with only slight increase in gravity values compared to the Amargosa Valley, which indicates a density more typical of a volcanic unit than an intrusion (table 1). Magnetic depth estimates using the gradient method indicate that the top to the magnetic source is 100-500 m below the surface and has a thick depth extent (depth extent is greater than depth to the top). Computation of gravity gradients show a linear, east-west gradient along the northern edge of the magnetic anomaly and extending a few kilometers to the west, suggesting fault control on this side.

Magnetic Expressions of Miscellaneous Volcanic Units

At Oasis Mountain (fig. 1; OM, fig. 6), a strong magnetic high corresponds well to topography and the mapped extent of the moderately magnetic rhyolite of Fleur-de-lis Ranch (Tff, table 2; fig. 15). To the west, a moderate positive anomaly corresponds to Ammonia Tanks Tuff (Tma, table 2) and topography. In between these two anomalies is a negative anomaly that is located at the unconformable boundary between the Fleur-de-lis Ranch rhyolite and the Ammonia Tanks Tuff. Its amplitude and extension to the south, where it is unrelated to topography, suggest the presence of a third unit having negative-inclination magnetization. The source of this negative anomaly is unknown, despite efforts to detect it on the ground.

At Springdale Mountain (fig. 1), mapped upper Fortymile rhyolite lavas (Tfu, table 2) have good correspondence to negative anomalies (SM, fig. 6; fig. 14) and topographic shapes. The trachyte of Donovan Mountain (Tfn, table 2) has good correspondence with positive anomalies and topographic shapes to the south, in the northern Bullfrog Hills (fig. 1; cf. fig. 5 and Carr and others, 1996 or Minor and others, in press). Because of the consistencies of these relations, the association of strong negative anomalies and mapped trachyte of Donovan Mountain on the east side of Springdale Mountain is contradictory and the geologic identification of this unit should be re-examined. It seems more likely that the upper Fortymile rhyolite lavas occur at the surface in this area. Moreover, the ribbon-like, strong positive anomaly trending north-south through Springdale Mountain corresponds to a steep topographic gradient, sloping to the west. Thus, the positive anomaly could be the expression of the trachyte of Donovan Mountain where it would underlie the upper Fortymile rhyolite lavas.

An elongate area of high-amplitude positive magnetic anomalies (BU, fig. 6) near the northeastern margin of the Ammonia Tanks caldera at Buckboard Mesa (fig. 11) corresponds to mapped basaltic trachyandesite of young Tertiary age (Typ, Table 2). The positive anomalies probably represent the thickest portion of the basalt (Kane and others, 1981). At the margins of the mapped basalt, the negative anomalies are probably due to underlying, older rocks.

A high-amplitude, negative magnetic anomaly (TR, fig. 6) is located just west of the Timber Mountain complex and just north of the Hot Springs fault (15, fig. 6). The anomaly corresponds in part to exposed Tram Tuff (Tct, table 2; fig. 15), which is about 150 m thick in this area (Fridrich, in press). It has strong negative-inclination total magnetization (table 2), as evidenced by the negative anomaly, except on the southwest, where it is hydrothermally altered (Kane and Bracken, 1983).

Notable on the magnetic map is the almost complete lack of magnetic anomalies on the eastern part of the pre-Tertiary high in the northern Bullfrog Hills (BH, fig. 6; fig. 5), despite the presence of mapped volcanic units in the area that elsewhere are highly magnetic, such as the Rainier Mesa tuff, the Tiva Canyon tuff, and the Bullfrog Tuff (Tmr, Tpc, and Tcb, respectively, table 2). However, the area has experienced multiple periods of hydrothermal alteration (Noble and others, 1991). Thus, the hydrothermal alteration probably destroyed much of the remanent magnetization in the rocks and thus significantly reduced their total magnetizations.

SUMMARY

New aeromagnetic data west of NTS have been integrated with new rock-property information, recent geologic mapping, and existing gravity and magnetic data to interpret subsurface features such as calderas, intrusions, basalt flows and volcanoes, Tertiary basins, structurally high pre-Tertiary rocks, and fault zones (fig. 6). Those features with major tectonic/magmatic significance are

(1) a north-south tectonic fault that bounds the west side of Oasis Valley basin and extends north of Sleeping Butte, which we call the Hogback fault (13, fig. 6; fig. 15);

(2) an east-striking transverse fault bounding the southern part of Oasis Valley basin on the east and extending west to the Bullfrog Hills, which we call the Hot Springs fault (15, fig. 6; fig. 15);

(3) a NNE-striking structural zone (6 and 7, fig. 6) that extends 25 km along the western limits of the Silent Canyon and Timber Mountain caldera complexes;

(4) a WNW-striking inferred structure near the northern margin of the Rainier Mesa caldera that may be related to the caldera;

(5) a 5-km thick pile of Tertiary rocks (RHN and RHS), probably consisting primarily of dacite lavas and tuffs, that is bounded by the previous two structures;

(6) a probable buried caldera southwest of Black Mountain (5, fig. 6) and possible source of the tuff of Tolicha Peak; and

(7) a possible buried caldera (4, fig. 7) south of Tolicha Peak that may be the source of the tuff of Sleeping Butte.

ACKNOWLEDGMENTS

We are grateful to Vicki Langenheim and Tom Hildenbrand, both of the USGS, for their detailed and helpful criticisms on geophysical interpretations; and to Randy Laczniak, Dave Ponce, Pete Rowley, all of the USGS, and Rick Warren (Los Alamos National Laboratories) for their review comments or informal input. We are especially indebted to Jim Cole (USGS), whose support, insight, and encouragement made this study possible.

REFERENCES CITED

Baranov, V., 1957, A new method for interpretation of aeromagnetic maps: pseudo-gravimetric anomalies: Geophysics. v. 22, p. 359-383.

Bath, G. D., 1968, Aeromagnetic anomalies related to remanent magnetism in volcanic rock, Nevada Test Site: Geol. Soc. America Memoir 110, p. 135-146.

Bath, G. D., and Jahren, C. E., 1984, Interpretation of magnetic anomalies at a potential repository site located in the Yucca Mountain areas, Nevada Test Site: U. S. Geological Survey Open-File Report 84-120, 40 p.

Blakely, R. J., 1995, Potential theory in gravity and magnetic applications: Cambridge University Press, 441 p.

Blakely, R. J., and Simpson, R. W., 1986, Approximating edges of source bodies from magnetic or gravity anomalies: Geophysics, v. 51, p. 1494-1498.

Byers, F. M., Jr., Carr, W. J., Orkild, P. P., Quinlivan, W. D., and Sargent, K. A., 1976a, Volcanic suites and related cauldrons of Timber Mountain-Oasis Valley caldera complex, southern Nevada: U. S. Geological Survey Professional Paper 919, 70 p.

Byers, F. M., Jr., Carr, W. J., Christiansen, R. L., Lipman, P. W., Orkild, P. P., and Quinlivan, W. D., 1976b, Geologic map of the Timber Mountain caldera area, Nye County, Nevada: U. S. Geological Survey Miscellaneous Investigations Map I-891, scale 1:48,000.

Carr, M. D., Sawyer, D. A., Nimz, Kathryn, Maldonado, Florian, and Swadley, WC, 1996, Digital bedrock geologic map database for the Beatty 30 x 60-minute quadrangle, Nevada and California: U. S. Geological Survey Open-File Report 96-291.

Carr, W. J., 1988, Volcano-tectonic setting of Yucca Mountain and Crater Flat, southwestern Nevada: U. S. Geological Survey Bulletin 1790, p. 35-49.

Carr, W. J., 1990, Styles of extension in the Nevada Test Site region, southern Walker Lane Belt; An integration of volcano-tectonic and detachment fault models: Geological Society of America Memoir 176, p. 283-303.

Carroll, R. D., 1989, Density logging and density of rocks in Rainier Mesa area, Nevada Test Site: U. S. Geological Survey Open-File Report 89-329, 252 p., 4 plates.

Christiansen, R. L., Lipman, P. W., Carr, W. J., Byers, F. M., Jr., Orkild, P. P., and Sargent, K. A., 1977, The Timber Mountain-Oasis Valley caldera complex of southern Nevada: Geological Society of America Bulletin, v. 88, p. 943-959.

Cordell, Lindrith, 1979, Gravimetric expression of graben faulting in Santa Fe country and the Espanola Basin, New Mexico: New Mexico Geol. Soc. Guidebook, 30th Field Conference, Santa Fe Country, p. 59-64.

Cordell, Lindrith, 1985, Techniques, applications, and problems of analytical continuation of New Mexico aeromagnetic data between arbitrary surfaces of very high relief [abs.]: Proceedings of the International Meeting on Potential Fields in Rugged Topography, Institute of Geophysics, University of Lausanne, Switzerland, Bulletin no. 7, p. 96-99.

Cordell, Lindrith, and Grauch, V. J. S., 1985, Mapping basement magnetization zones from aeromagnetic data in the San Juan Basin, New Mexico *in* Hinze, W. J., ed., The utility of regional gravity and magnetic anomaly maps: Society of Exploration Geophysicists, Tulsa, Oklahoma, p. 181-197.

Cordell, Lindrith, and Henderson, R. G., 1968, Iterative three-dimensional solution of gravity anomaly data using a digital computer: Geophysics, v. 33, p. 596-601.

Cordell, Lindrith, and McCafferty, A. E., 1989, A terracing operator for physical property mapping with potential field data: Geophysics, v. 54, no. 5, p. 621-634.

Cornwall, H. R., 1972, Geology and mineral deposits of southern Nye County, Nevada: Nevada Bureau of Mines and Geology Bulletin 77, 49 p., 2 plates.

Ferguson, J. F., Cogbill, A. H., And Warren, R. G., 1994, A geophysical-geological transect of the Silent Canyon caldera complex, Pahute Mesa, Nevada: Journal of Geophysical Research, v. 99, no. B3, p. 4323-4339.

Fleck, R. J., Turrin, B. D., Sawyer, D. A., Warren, R. G., Champion, D. E., Hudson, M. R., and Minor, S. A., 1996, Age and character of basaltic rocks of the Yucca Mountain region, southern Nevada: Journal of Geophysical Research, v. 101, no. B4, p. 8205-8227.

Fridrich, C. J., in press, Tectonic evolution of the Crater Flat basin, Yucca Mountain region, Nevada: Geological Society of America Special paper, L. A. Wright and B. W. Troxel, eds., Cenozoic Basins of the Death Valley region.

Furgerson, R. B., 1982, Remote-reference magnetotelluric survey Nevada Test Site and vicinity, Nevada and California: U. S. Geological Survey Open-File Report 82-465, 145 p., 2 plates.

Grauch, V. J. S., 1987a, The importance of total magnetization in aeromagnetic interpretation of volcanic areas; An illustration from the San Juan Mountains, Colorado: Expanded abstracts with biographies, 57th Annual International Society of Exploration Geophysicists meeting, Oct. 11-15, 1987, p. 109-110.

Grauch, V. J. S., 1987b, A new variable-magnetization terrain correction method for aeromagnetic data: Geophysics, v. 52, p. 94-107.

Grauch, V. J. S., and Cordell, Lindrith, 1987, Limitations of determining density or magnetic boundaries from the horizontal gradient of gravity or pseudogravity data: Geophysics, v. 52, no. 1, p. 118-121.

Grauch, V. J. S., Kucks, R. P., and Bracken, R. E., 1993, Aeromagnetic data for western areas of the Pahute Mesa and Beatty 30 X 60 minute quadrangles, Nye County, Nevada: EROS Data Center Magnetic Tape A0804, Sioux Falls, South Dakota.

Harris, R. N., Ponce, D. A., Healey, D. L., and Oliver, H. W., 1989, Principal facts for about 16,000 gravity stations in the Nevada Test Site and vicinity: U. S. Geological survey Open-file Report 89-682a-c.

Healey, D. L., 1968, Application of gravity data to geologic problems at the Nevada Test Site: Geological Society of America Memoir 110, p. 147-156.

Healey, D. L., 1983, Gravity investigations *in* Geologic and geophysical investigations of Climax Stock intrusive, Nevada: U. S. Geological Survey Open-File Report 83-377, p. 25-39.

Healey, D. L., Clutsom, F. G., and Glover, D. A., 1984, Borehole gravity meter surveys in drill holes USW G-3, UE-25p#1 and UE-25c#1, Yucca Mountain area, Nevada: U. S. Geological Survey open-File Report 84-672, 16 p.

Hudson, M. R., Minor, Scott A., Fridrich, C. J., 1996, The distribution, timing, and character of steep-axis rotations in a broad zone of dextral shear in southwestern Nevada: Geological Society of America Abstracts with Programs, v. 28, no. 7, p. 451.

Jachens, R. C., and Moring, B. C., 1990, Maps of the thickness of Cenozoic deposits and the isostatic residual gravity over basement for Nevada: U. S. Geological Survey Open-File Report 90-404, 15 p., 2 plates.

Jachens, R. C., Moring, B. C., and Schruben, P. G., 1996, Thickness of Cenozoic deposits and the isostatic residual gravity over basement for Nevada, in Singer, D. A., ed., An analysis of Nevada's metal-bearing mineral resources: Nevada Bureau of Mines and Geology Open-File Report 96-2, p. 2-1 through 2-10, 1 plate, scale 1:1,000,000.

Kane, M. F., and Bracken, 1983, Aeromagnetic map of Yucca Mountain and surrounding regions, southwestern Nevada: U. S. Geological Survey Open-File Report 83-616, 19 p.

Kane, M. F., Webring, M. W., and Bhattacharyya, B. K., 1981, A preliminary analysis of gravity and aeromagnetic surveys of the Timber Mountain area, southern Nevada: U. S. Geological Survey Open-File Report 81-189, 40 p., 6 plates.

Klein, D. P., 1995, Regional magnetotelluric investigations, *in* Oliver, H. W., Ponce, D. A., and Hunter, W. C., Eds., Major results of geophysical investigations at Yucca Mountain and vicinity, southern Nevada: U. S. Geological Survey Open-File Report 95-74, p. 73-97.

Laczniak, R., Cole, J.C., Sawyer, D.A., and Trudeau, D., 1996, Summary of hydrogeologic controls on ground-water flow at the Nevada Test Site, Nye County, Nevada: U.S. Geological Survey Water-Resources Investigation Report 96-4109, 59 p.

Langenheim, V. E., in press, Constraints on the structure of Crater Flat, southwest Nevada, derived from gravity and magnetic data, *in* Whitney, J. W., ed., Tectonics and seismic hazard at Yucca Mountain, Nevada: U. S. Geological Survey Circular.

Langenheim, V. E., Carle, S. F., Ponce, D. A., and Phillips, J. D., 1991, Revision of an aeromagnetic survey of the Lathrop Wells area, Nevada: U. S. Geological Survey Open-File Report 91-46, 17 p.

Larson, E., Ozima, Mituko, Ozima, Minoru, Nagata, T., and Strangway, D., 1969, Stability of remanent magnetization of igneous rocks: Geophysical Journal of the Royal Astronomical Society, v. 17, p. 263-292.

McCafferty, A. E., and Grauch, V. J. S., 1997, Aeromagnetic and gravity anomaly maps of the southwestern Nevada volcanic field, Nevada and California: U. S. Geological Survey Geophysical Investigations Map GP-1015, 1:250,000. [Digital data available from National Geophysical Data Center, Boulder, Colorado]

McElhinny, M. W., 1973, Paleomagnetism and plate tectonics: Cambridge University Press, Cambridge, England, 358 p.

Minor, S. A., Orkild, P. P., Swadley, WC, Warren, R. G., and Workman, J. B., in press, Preliminary digital geologic map of the Springdale quadrangle, Nevada: U. S. Geological Survey Open-File Report

Minor, S. A., Vick, G. S., Carr, M. D., Wahl, R. R., 1996, Faults, lineaments, earthquake epicenters digital map of the Pahute Mesa 30' X 60' quadrangle, Nevada: U. S. Geological Survey Open-File Report 96-262, 13 p., 1:100,000 scale.

Noble, D. C., Weiss, S. I., and McKee, E. H., 1991, Magmatic and hydrothermal activity, caldera geology, and regional extension in the western part of the southwestern Nevada volcanic field, *in* Raines, G. L., Lisle, R. E., Schafer, R. W., and Wilkinson, W. H., eds., Geology and ore deposits of the Great Basin, Symposium Proceedings: Geological Society of Nevada, Reno, Nevada, p. 913-934.

Oliver, H. W., and Fox, K. F., 1993, Structure of Crater Flat and Yucca Mountain, southeastern Nevada, as inferred from gravity data: American Nuclear Society Proceedings of the Fourth Annual International Conference on High Level Nuclear Waste Management, April 26-30, 1993, Las Vegas, NV, v. 2, p. 1812-1817.

Oliver, H. W., Ponce, D. A., and Hunter, W. C., Eds., 1995, Major results of geophysical investigations at Yucca Mountain and vicinity, southern Nevada: U. S. Geological Survey Open-File Report 95-74, 184 p.

Orkild, P. P., Byers, F. M., Jr., Hoover, D. L., and Sargent, K. A., 1968, Subsurface geology of Silent Canyon caldera, Nevada Test Site, Nevada: Geological Society of America Memoir 110, p. 77-86.

Phillips, J. A., and Grauch, V. J. S., Eds., in press, Geophysical map interpretation on the PC--A self-paced course using USGS potential-field and imaging software packages and geophysical data for the Getchell gold trend area, Osgood Mountains, Nevada: U. S. Geological Survey Digital series DDS-.

Plouff, Donald, and Pakiser, L. C., 1972, Gravity study of the San Juan Mountains, Colorado: U. S. Geological Survey Professional Paper 800-B, p. B183-B190.

Ponce, D. A., and Oliver, H. W., 1995, Gravity investigations, *in* Oliver, H. W., Ponce, D. A., and Hunter, W. C., Major results of geophysical investigations at Yucca Mountain and vicinity, southern Nevada: U. S. Geological Survey Open-File Report 95-74, p. 33-53.

Rosenbaum, J. G., and Snyder, D. B., 1984, Preliminary interpretation of paleomagnetic and magnetic property data from drill holes USW G-1, GU-3, G-3, and VH-1 and surface localities in the vicinity of Yucca Mountain, Nye County, Nevada: U. S. Geological Survey Open-File Report 85-49, 73 p.

Saltus, R. W., 1988a, Bouguer gravity anomaly map of Nevada: Nevada Bureau of Mines and Geology Map 94A, scale 1:750,000.

Saltus, R. W., 1988b, Regional, residual, and derivative gravity maps of Nevada: Nevada Bureau of Mines and Geology Map 94B, scale 1:750,000.

Saltus, R. W., and Jachens, R. C., 1995, Gravity and basin-depth maps of the Basin and Range province, western United States: U. S. Geological Survey Geophysical Investigations Map GP-1012, 1:2,500,000 scale.

Sawyer, D. A., Fleck, R. J., Lanphere, M. A., Warren, R. G., Broxton, D. E., and Hudson, M. R., 1994, Episodic caldera volcanism in the Miocene southwestern Nevada volcanic field: Revised stratigraphic framework, $^{40}Ar/^{39}Ar$ geochronology, and implications for magmatism and extension: Geological Society of America Bulletin, v. 106, p. 1304-1318.

Sawyer, D.A., Wahl, R.R., Cole, J.C., Minor, S.A., Laczniak, R.J., Warren, R.G., Engle, C.M., and Vega, R.G., 1995, Preliminary digital geologic map database of the Nevada Test Site area, Nevada: U.S. Geological Survey Open-file Report 95-0567, scale 1:130,000 and digital data.

Sawyer, D. A., and Sargent, K. A., 1989, Petrologic evolution of divergent peralkaline magmas from the Silent Canyon caldera complex, southwestern Nevada volcanic field: Journal of Geophysical Research, v. 94, no. B5, p. 6021-6040.

Simpson, R. W., and Jachens, R. C., 1989, Gravity methods in regional studies: Geological Society of America Memoir 172, p. 35-44.

Smith, R. L., and Bailey, R. A., 1968, Resurgent cauldrons: Geological Society of America Memoir 116, p. 613-662.

Snyder, D. B., and Carr, W. J., 1982, Preliminary results of gravity investigations at Yucca Mountain and vicinity, southern Nye County, Nevada: U. S. Geological Survey Open-File Report 82-701, 36 p., 1 plate.

Snyder, D. B., and Carr, W. J., 1984, Interpretation of gravity data in a complex volcano-tectonic setting, southwestern Nevada: Journal of Geophysical Research, v. 89, no. B12, p. 10,193-10,206.

Warren, R.G., Byers, F.M., and Orkild, P.P, 1985, Post-Silent Canyon caldera structural setting for Pahute Mesa *in* Olsen, C. W., and Carter, J. A., eds., Fifth Symposium on Containment of Underground Nuclear Explosions--vol. 2: Lawrence Livermore National Laboratory Mission Research Corp. Report CONF-850953, v. 2, p. 31-45.

Warren, R. G., Sawyer, D. A., and Covington, H. R., 1989, Revised volcanic stratigraphy of the southwestern Nevada volcanic field, Fifth Symposium on Containment of Underground Nuclear Explosions, Lawrence Livermore National Laboratory, CONF-8909163, p. 33.

Zablocki, C. J., 1979, Some reconnaissance-type electrical surveys of Timber Mountain caldera, Nye County, Nevada: U. S. Geological Survey Open-File Report 79-1695, 23 p.

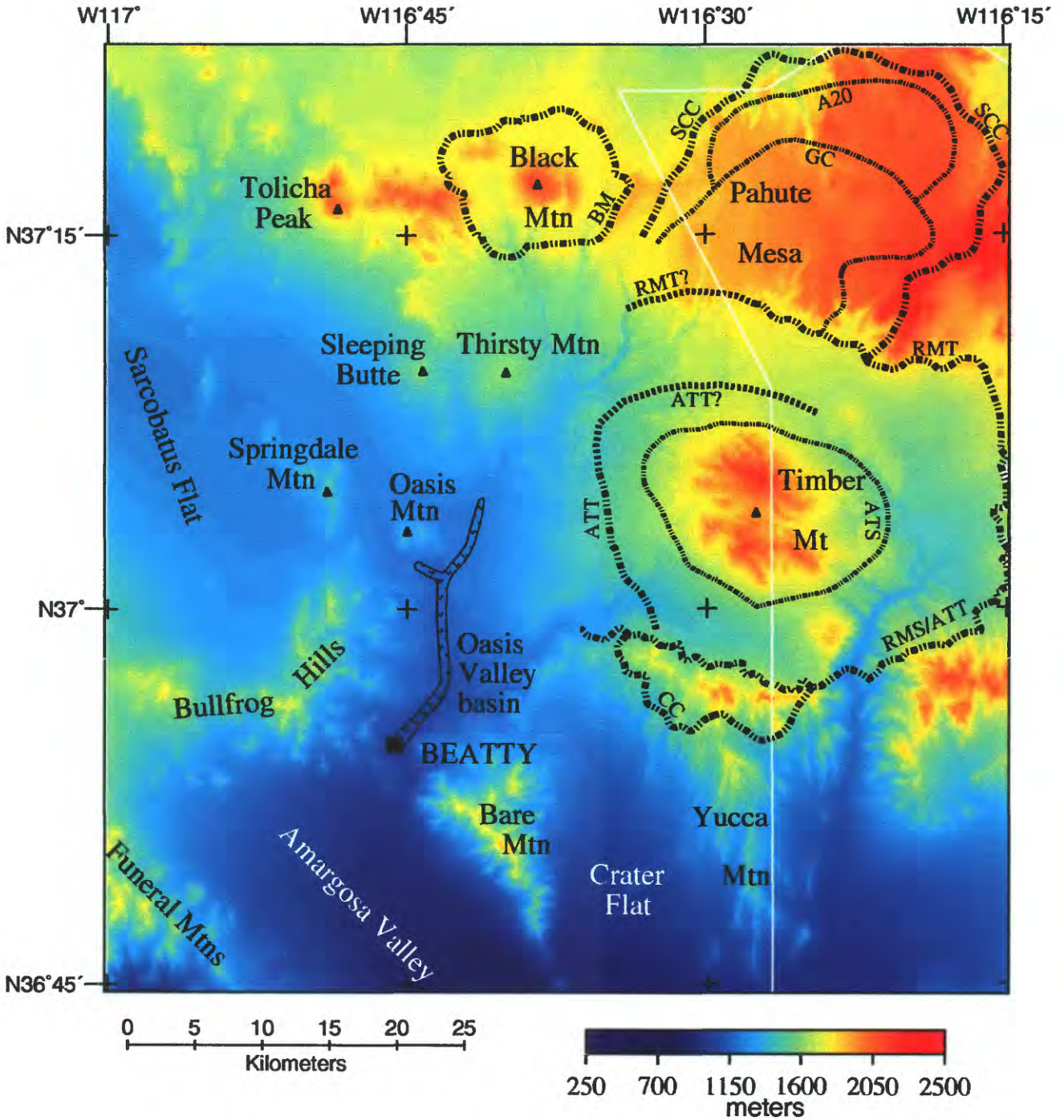

Figure 1 - Map showing topography of the study area. Also shown are caldera topographic margins (thick dash-dot-dot line where well defined, thick short-dash line where poorly defined) of the Ammonia Tanks (ATT), Black Mountain (BM), Claim Canyon (CC), Rainier Mesa (RMT) calderas and Silent Canyon caldera complex (SCC); and caldera structural margins (medium-thick dash-dot-dot line) of the Ammonia Tanks (ATS), Area 20 (A20), Grouse Canyon (GC), and Rainier Mesa (RMS) calderas. The white line is the Nevada Test Site (NTS) boundary and the V pattern is Oasis Valley discharge area.

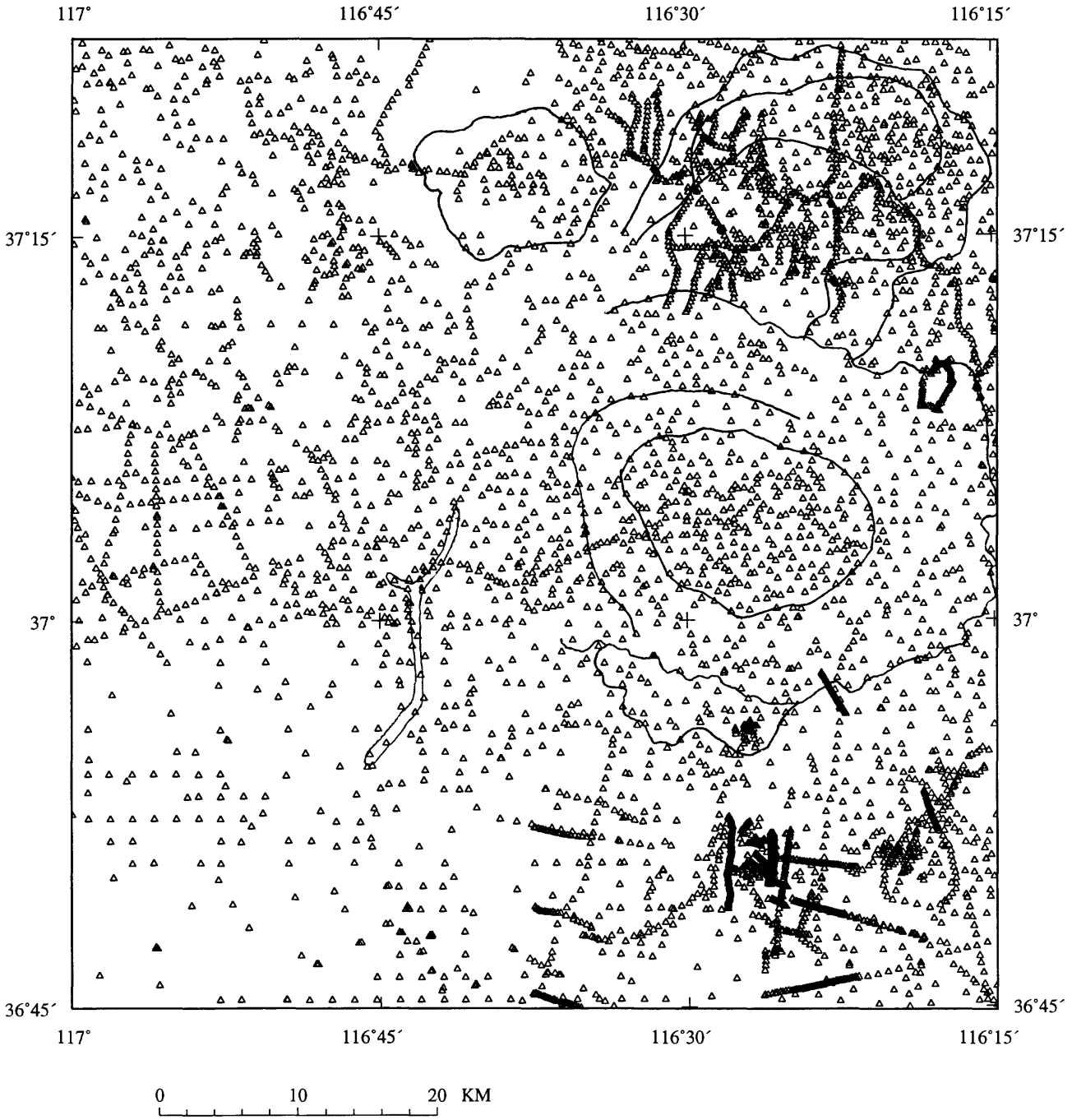

Figure 2 - Gravity station locations (small triangles) in the study area. Caldera outlines from figure 1 are shown as thin solid lines.

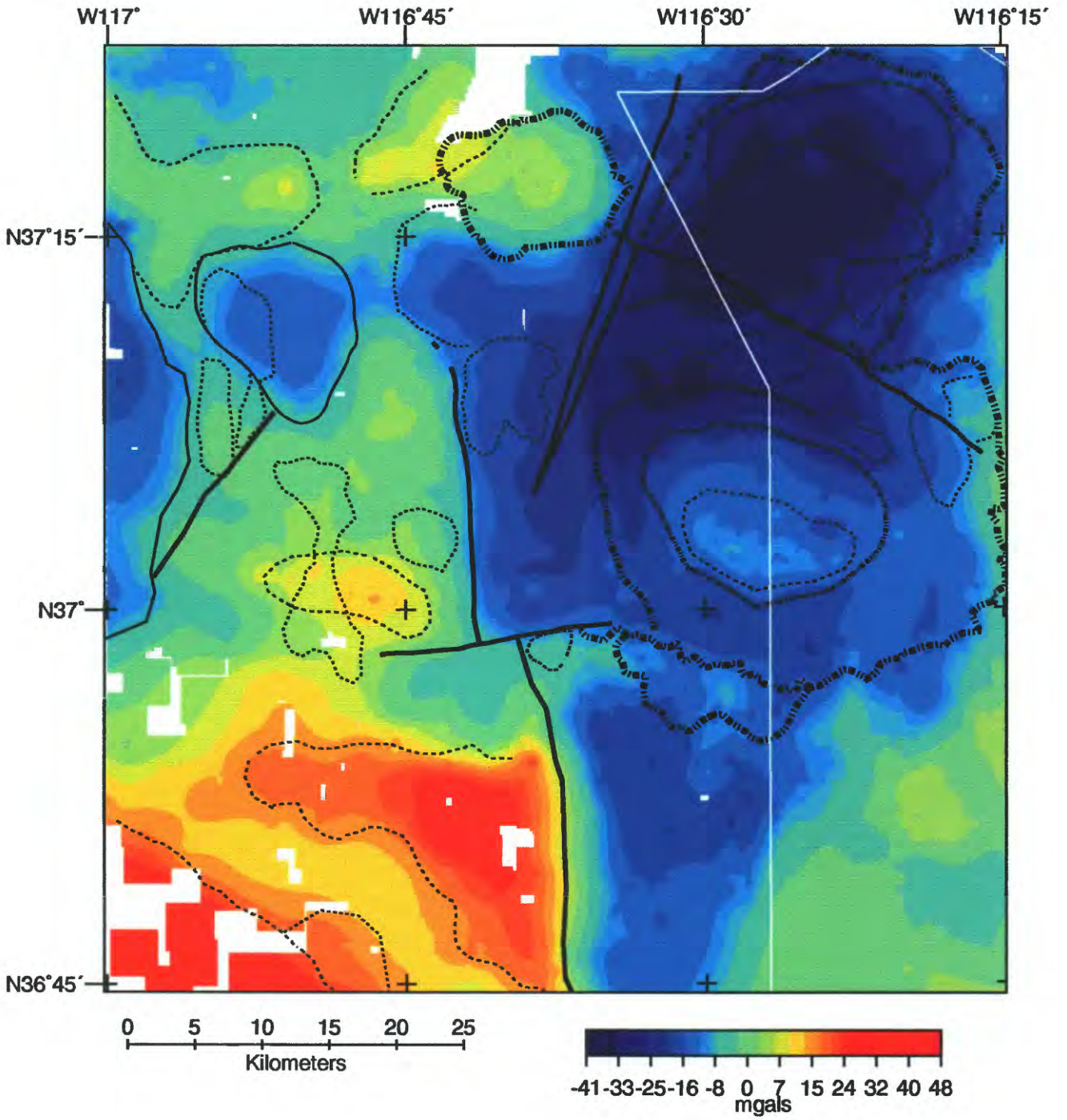

Figure 3 - Color isostatic residual gravity map based on a reduction density of 2400 kg/m^3 (see text for discussion). White areas show where data coverage was too coarse for interpolation. Some artifacts due to "bad" stations are still apparent in the data set as circular features less than 1 km in diameter, such as the artifact at the northeastern corner of Bare Mountain (cf. fig. 1). Due to the enormous number of data points involved (Harris and others, 1989), time was not available to resolve all the data problems. The boundary of NTS is shown by the white line. Black dashed and solid lines are outlines of caldera margins (fig. 1) and interpreted features shown in figure 6 and discussed in text.

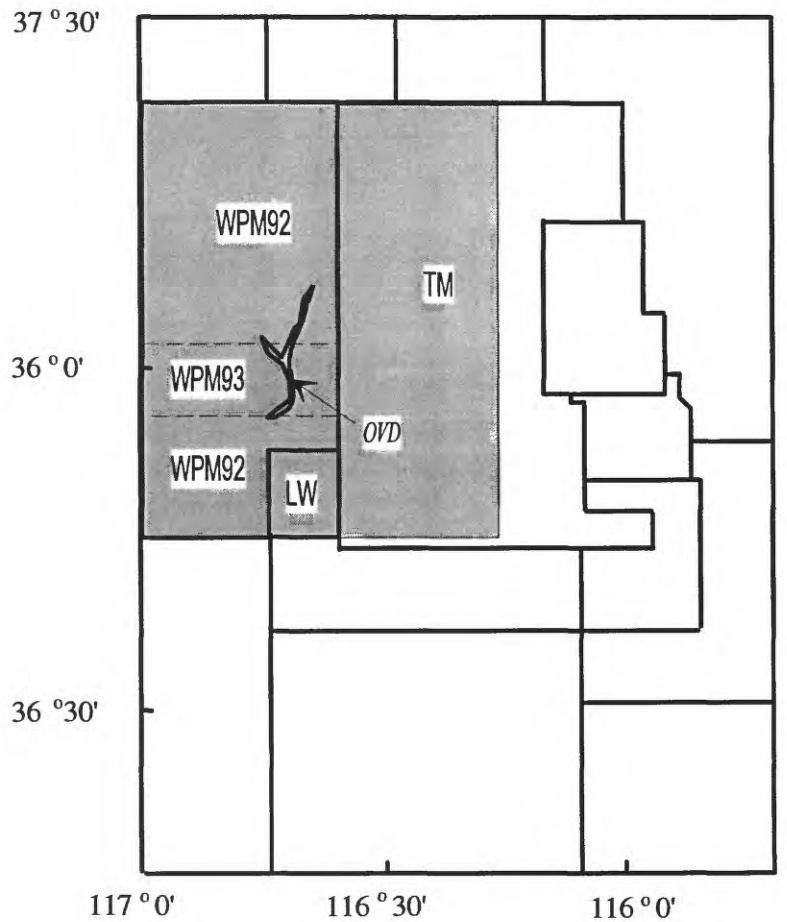

———	Aeromagnetic survey boundary
WPM92	West Pahute Mesa survey, flown November 1992
WPM93	West Pahute Mesa survey, flown April 1993
TM	Timber Mountain survey
LW	Lathrop Wells survey, flown with north-south lines

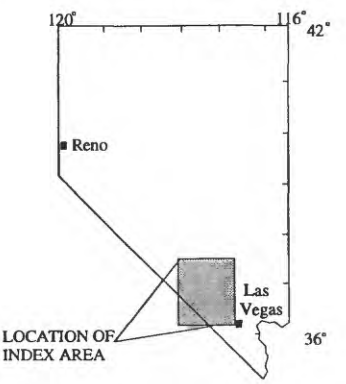

Figure 4 - Index map of aeromagnetic surveys, showing those used in the compilation of McCafferty and Grauch (1997) and those covering the study area (shading). The West Pahute Mesa (Grauch and others, 1993) and Timber Mountain (Kane and others, 1981) surveys were flown 122 m above ground along east-west flight lines spaced 400 m apart. The Lathrop Wells survey (Langenheim and others, 1991) was flown at 300 m above ground along north-south flight lines spaced 800 m apart. It was part of a larger survey, most of which was flown with east-west lines. OVD, Oasis Valley discharge area.

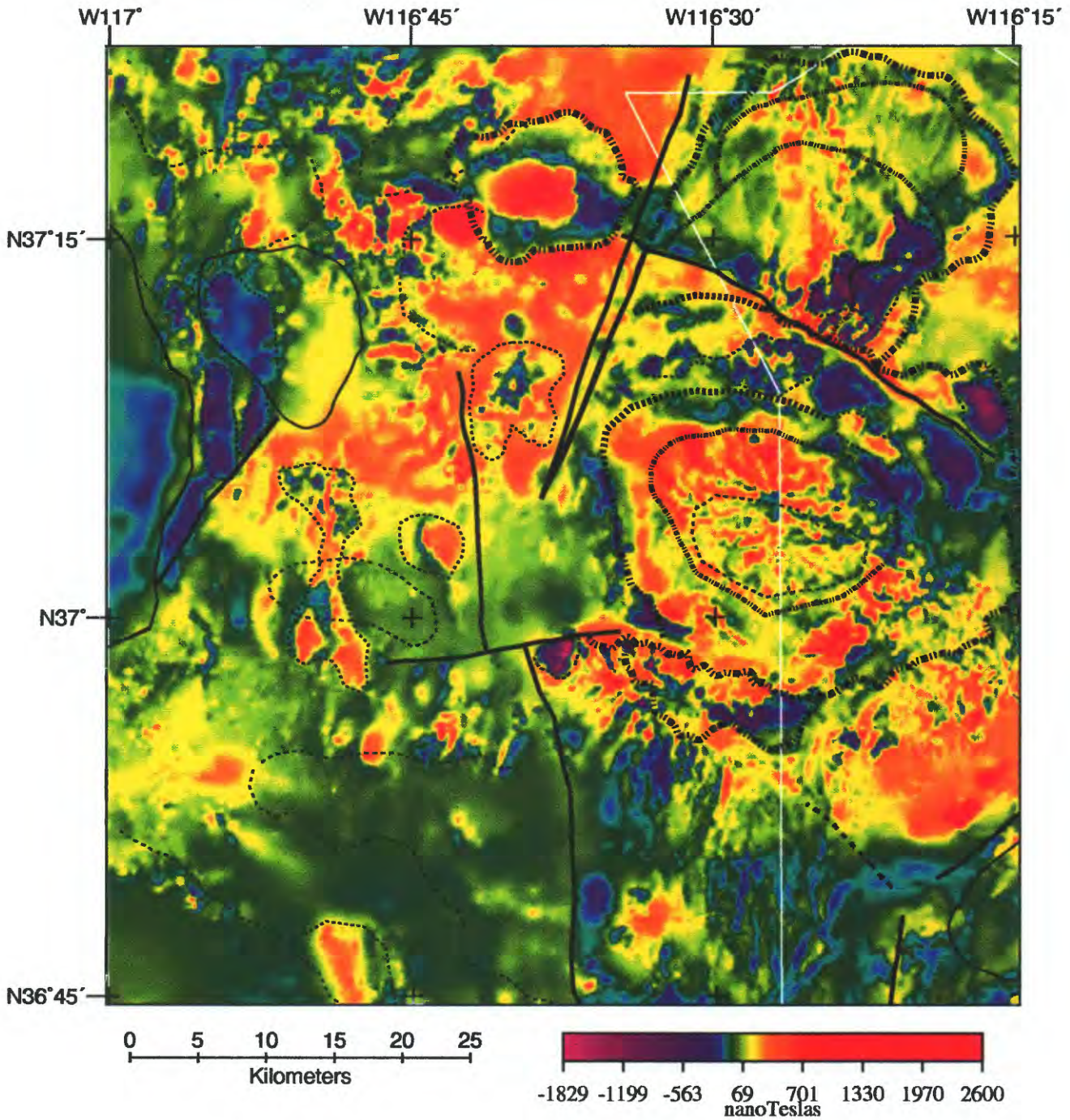

Figure 5 - Color reduced-to-pole aeromagnetic map. The boundary of NTS is shown by the white line. Black dashed and solid lines are outlines of caldera margins (fig. 1) and interpreted features shown in figure 6 and discussed in text.

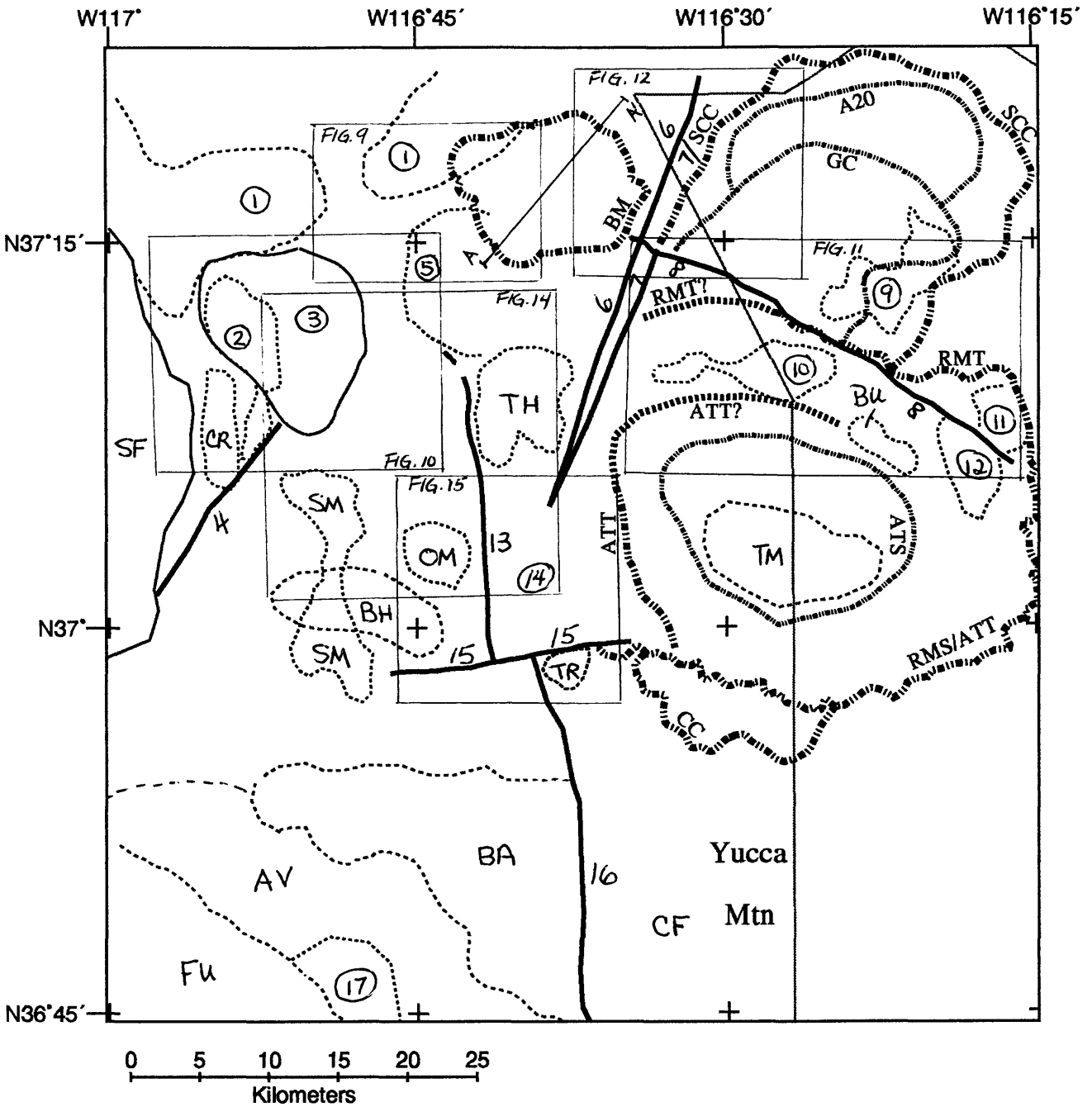

Figure 6 - Outlines of interpreted subsurface features with code letters and numbers that are referred to in text. Outlines are also overlain on figures 3 and 5. Code letters refer to geologic features that have geophysical expression; numbers to features inferred in the subsurface. Major interpreted faults are shown by thick solid lines; interpreted basins are outlined with thin solid lines and other features with thin dashed lines.. Also shown are caldera topographic margins (thick dash-dot-dot line where well defined, thick short-dash line where poorly defined) of the Ammonia Tanks (ATT), Black Mountain (BM), Claim Canyon (CC), Rainier Mesa (RMT) calderas and Silent Canyon caldera complex (SCC); and caldera structural margins (medium-thick dash-dot-dot line) of the Ammonia Tanks (ATS), Area 20 (A20), Grouse Canyon (GC), and Rainier Mesa (RMS) calderas. The rectangles on the figure refer to the locations of areas shown in figures 9, 10, 11, 12, 14, and 15. NTS boundary is the solid dark gray line. Geophysical data were not interpreted in the area of Yucca Mountain.

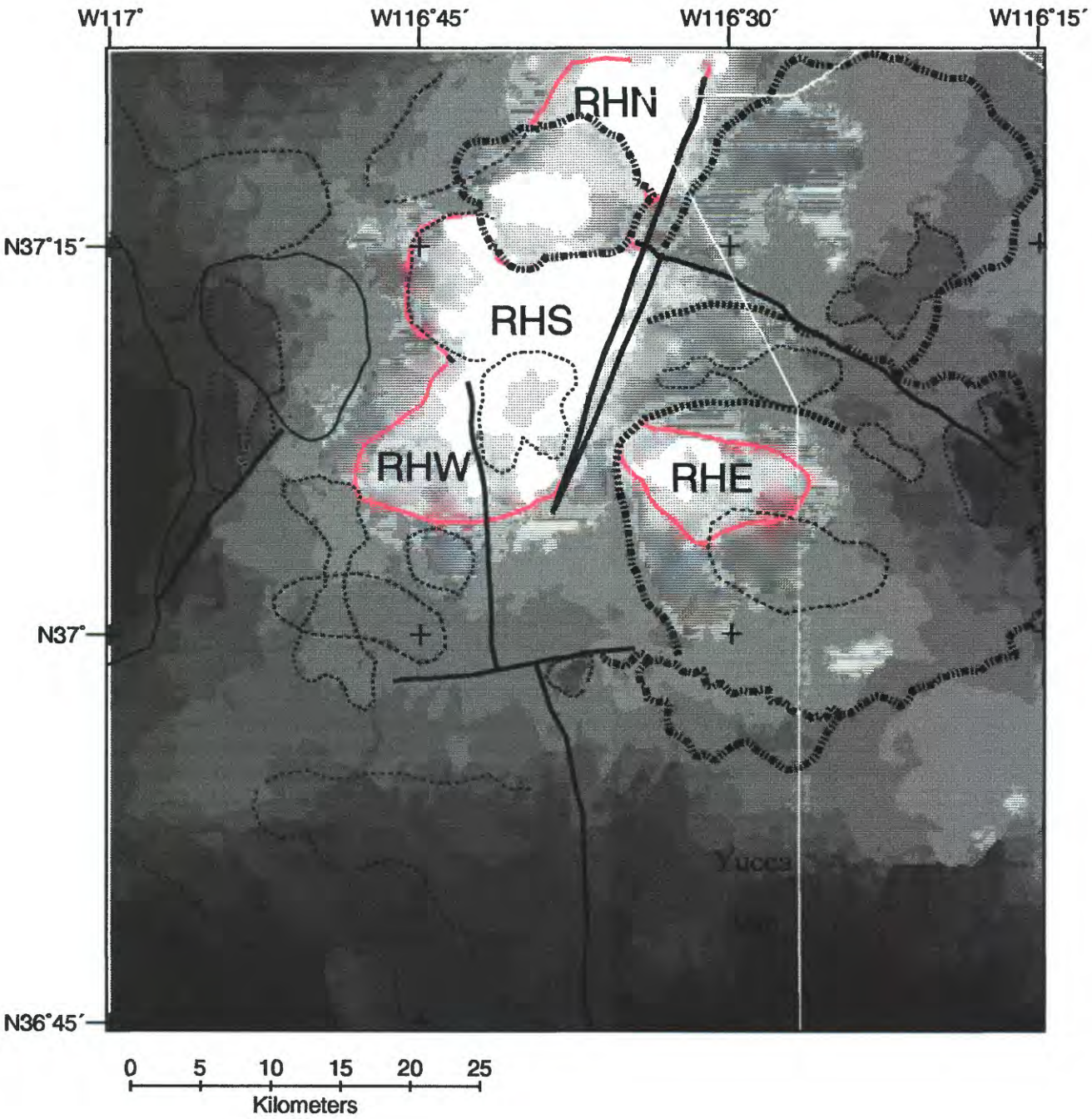

Figure 7 - Graytone map of magnetic potential (pseudogravity) data to which the terracing operator of Cordell and McCafferty (1989) has been applied. Also shown are outlines of interpreted features and calderas from figure 6. The magnetic-potential map can be viewed as an indicator of the relative values of bulk magnetization of the upper crust. High values correspond to light tones; low values to dark tones. Units are not shown because the values are only relative. Bulk magnetization of the upper crust is not well represented in areas where strong negative magnetic anomalies have wide lateral extent, such as feature 2 on the west and features 9, 11, and 12 on the east (cf. figs. 5 and 6). Areas of regionally high values are outlined in pink (RHN, RHS, RHW, and RHE) and discussed in text. NTS boundary is shown in white.

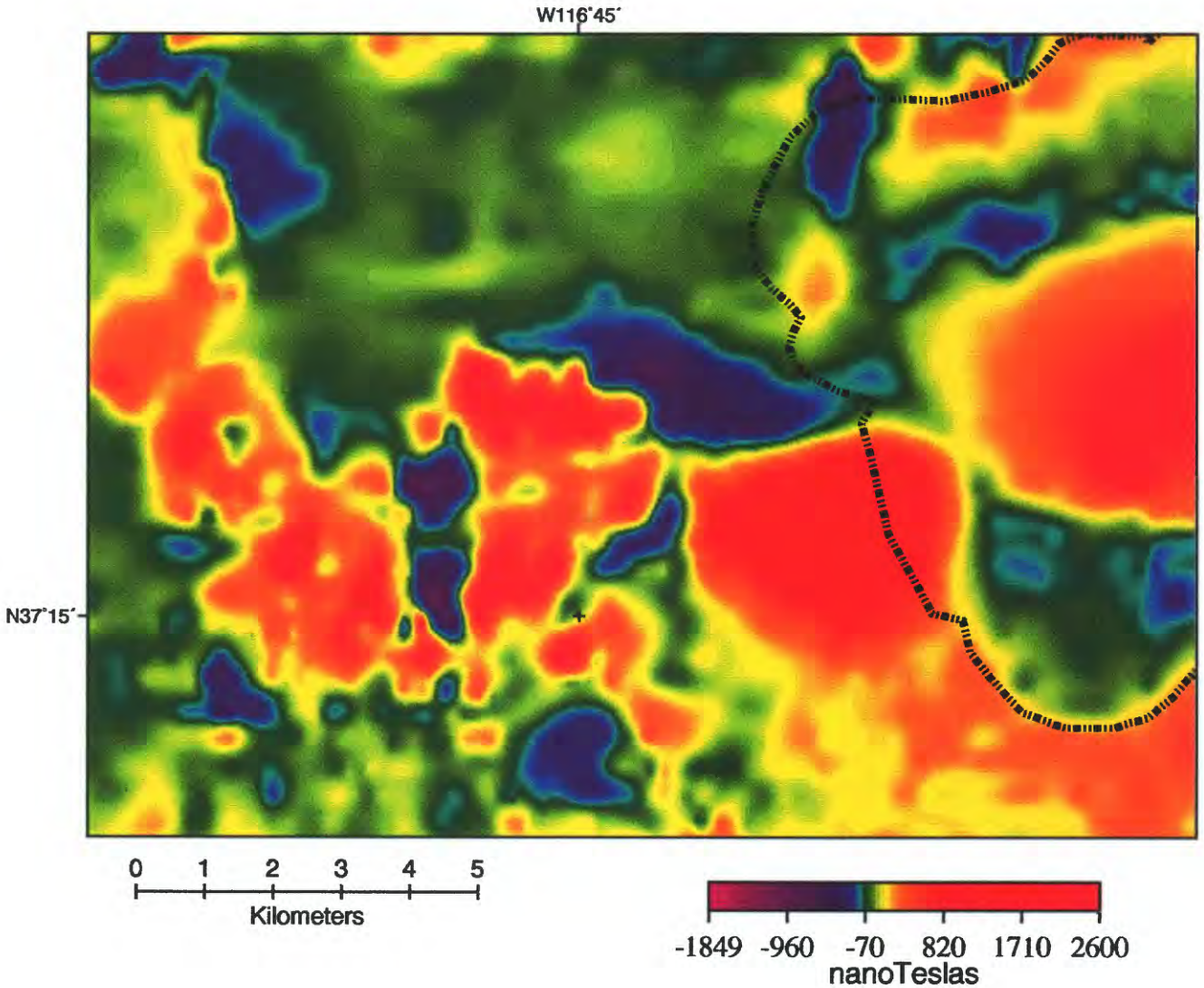

Figure 8b - Reduced-to-pole magnetic map for western Black Mountain caldera (thick dash-dot-dot line) and vicinity. Location of area shown on figure 6. Geologic overlay is figure 8a in pocket.

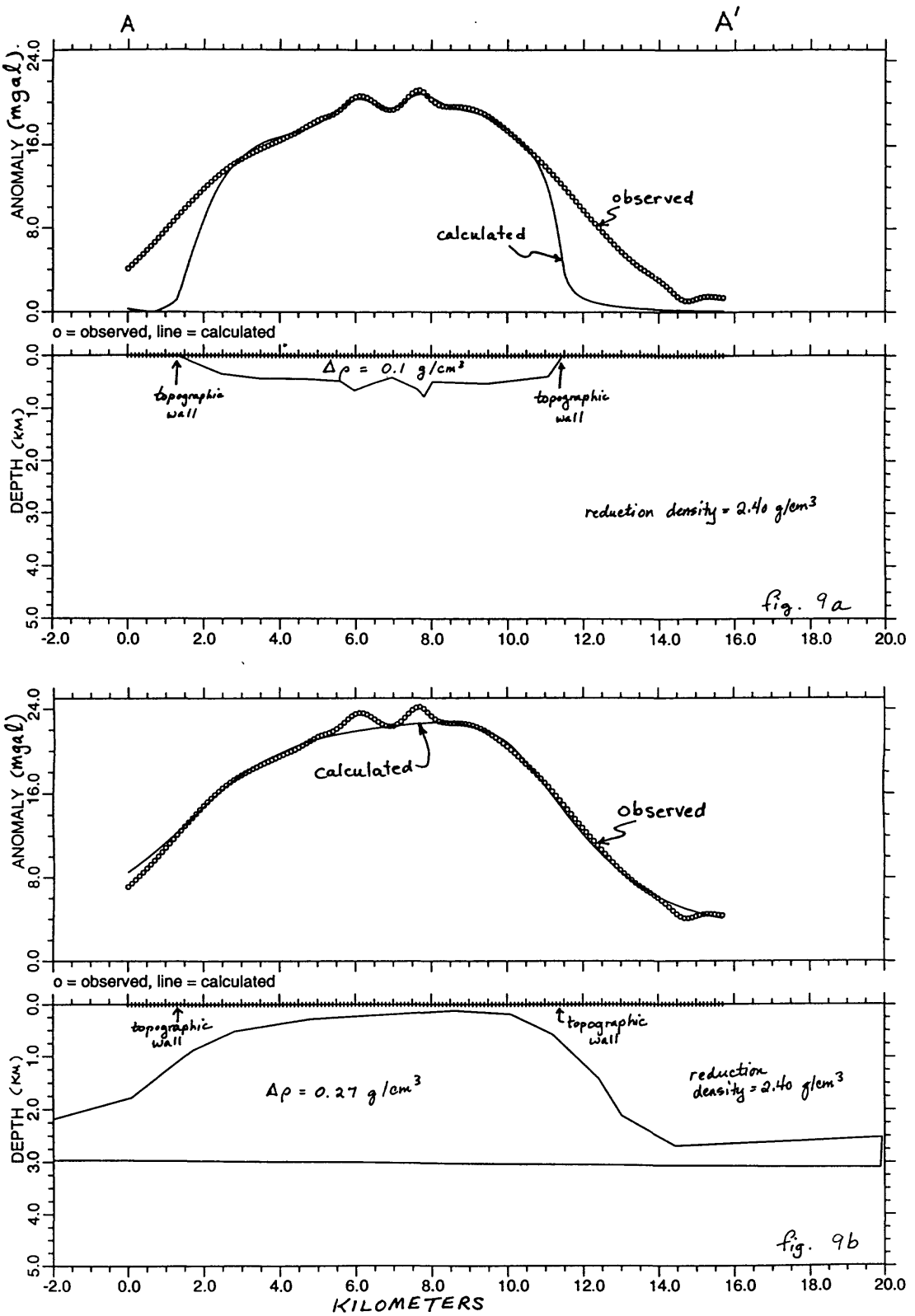

Figure 9 - Simple gravity models for profile A-A' (located on fig. 6) across Black Mountain caldera. A model of high-density caldera fill (a) cannot entirely account for the lateral extent of the observed gravity anomaly, because the caldera fill is bounded by the caldera topographic walls. A simple model of an intrusion (b) demonstrates that a moderate-density intrusion can explain the breadth of the gravity high.

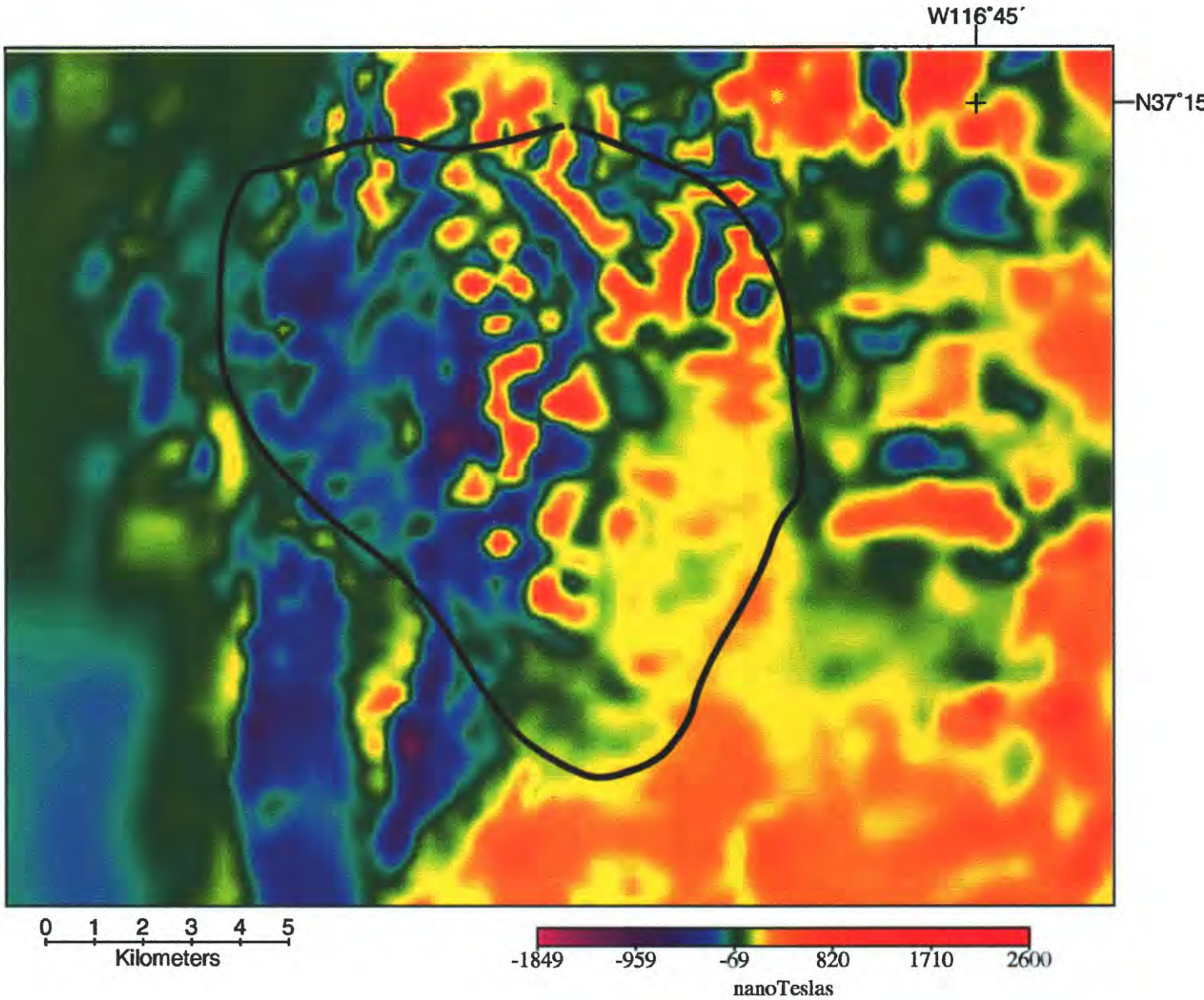

Figure 10b - Reduced-to-pole magnetic map continued down within the area of the elliptical gravity low (black line; 4, fig. 6) west of Sleeping Butte. The data were continued onto a surface with maximum depth of 500 m in the center, discussed in text. This procedure enhances the character of anomalies due to volcanic units at lower elevations. Location of area shown on figure 6. Geologic overlay is figure 10a in pocket.

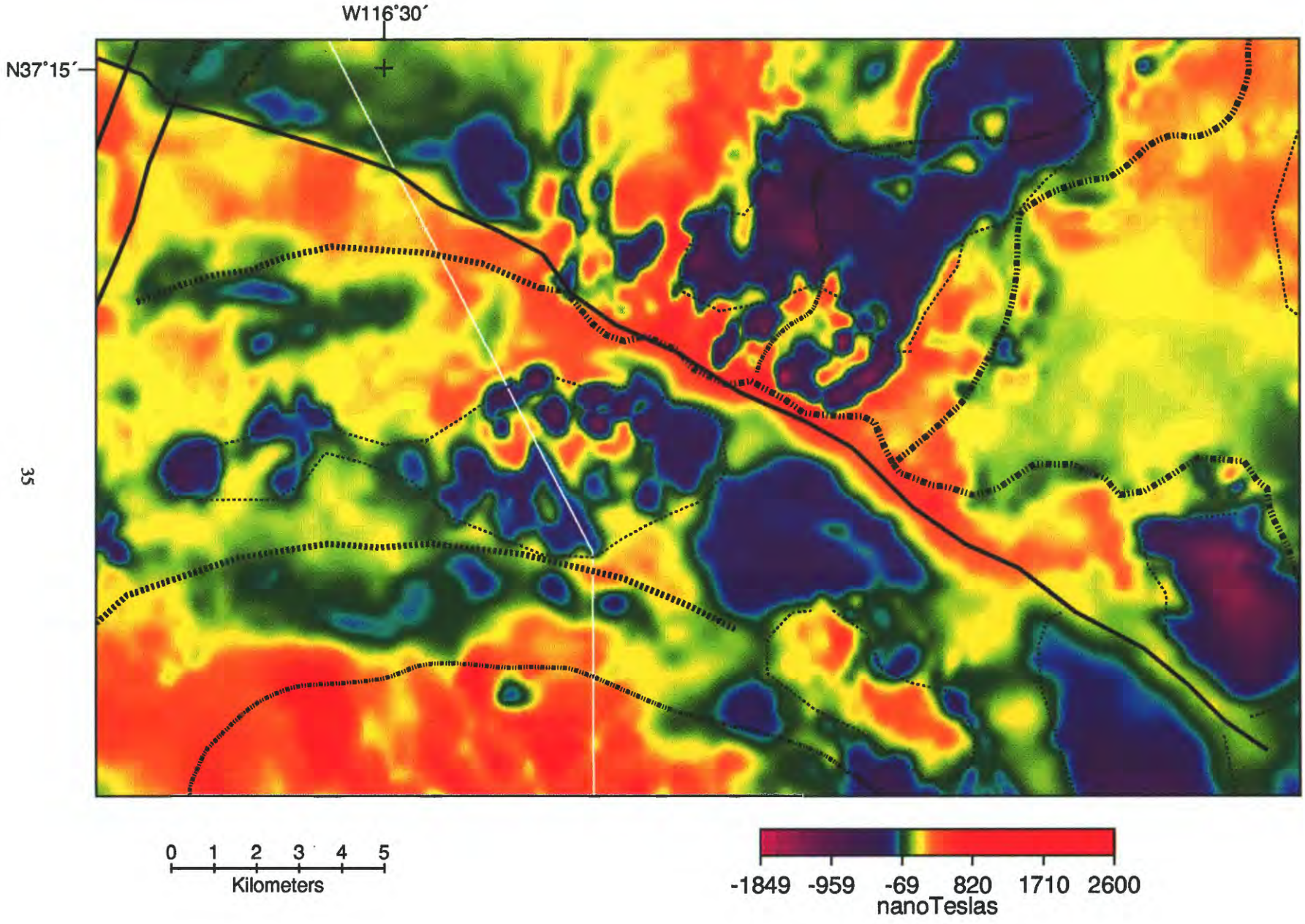

Figure 11b - Reduced-to-pole magnetic map of the northern part of Rainier Mesa caldera and Pahute Mesa, showing features and caldera margins from figure 6. Location of area shown on figure 6. Geologic overlay is figure 11a in pocket.

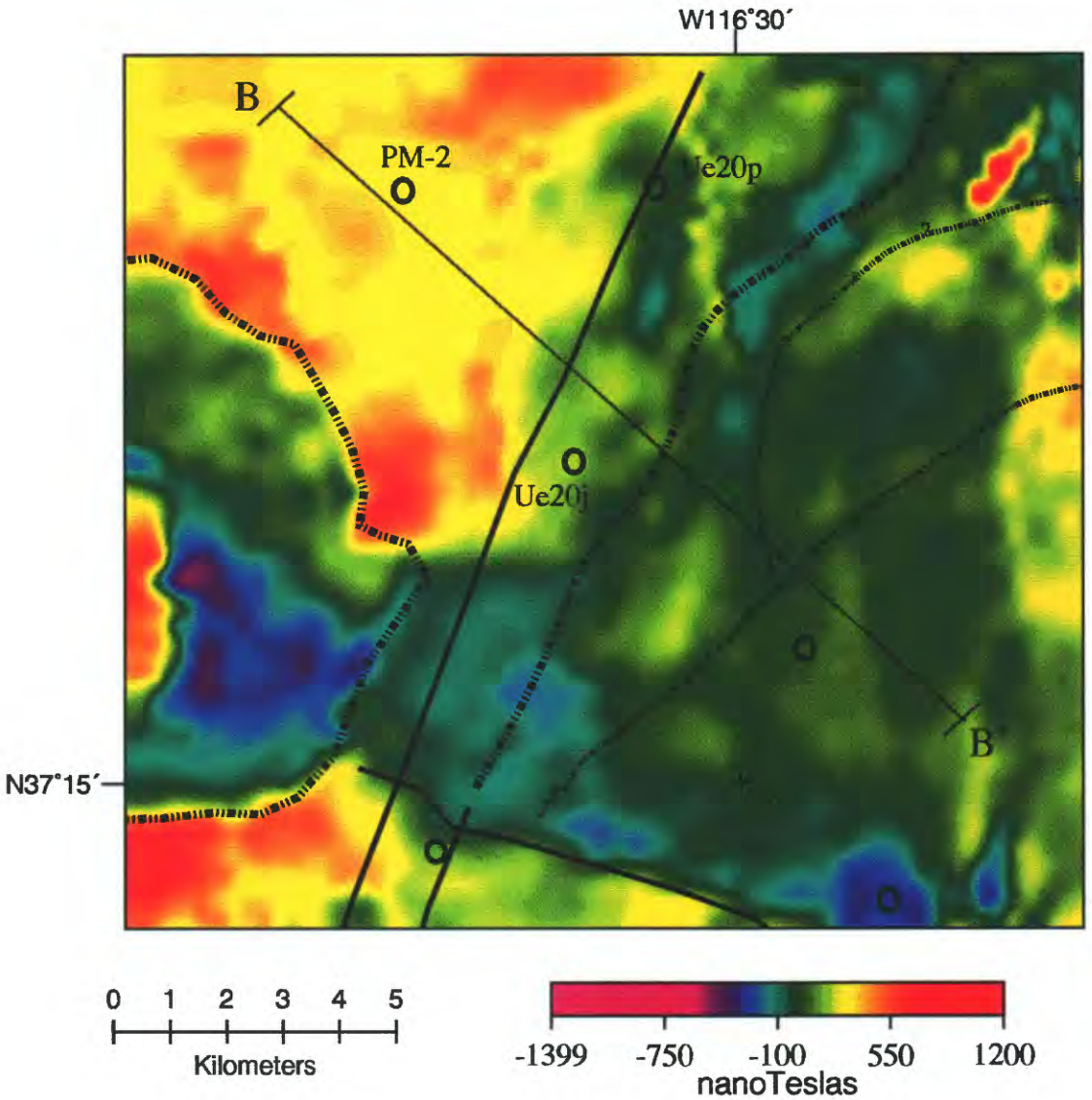

Figure 12b - Reduced-to-pole magnetic map showing western Pahute mesa, eastern Black Mountain caldera (thick dash-dot-dot line), and features from figure 6. Drill holes are shown by the bold open circles; those discussed in text are labeled. Profile B-B' is described in figure 13. Location of area shown on figure 6. Geologic overlay is figure 12a in pocket.

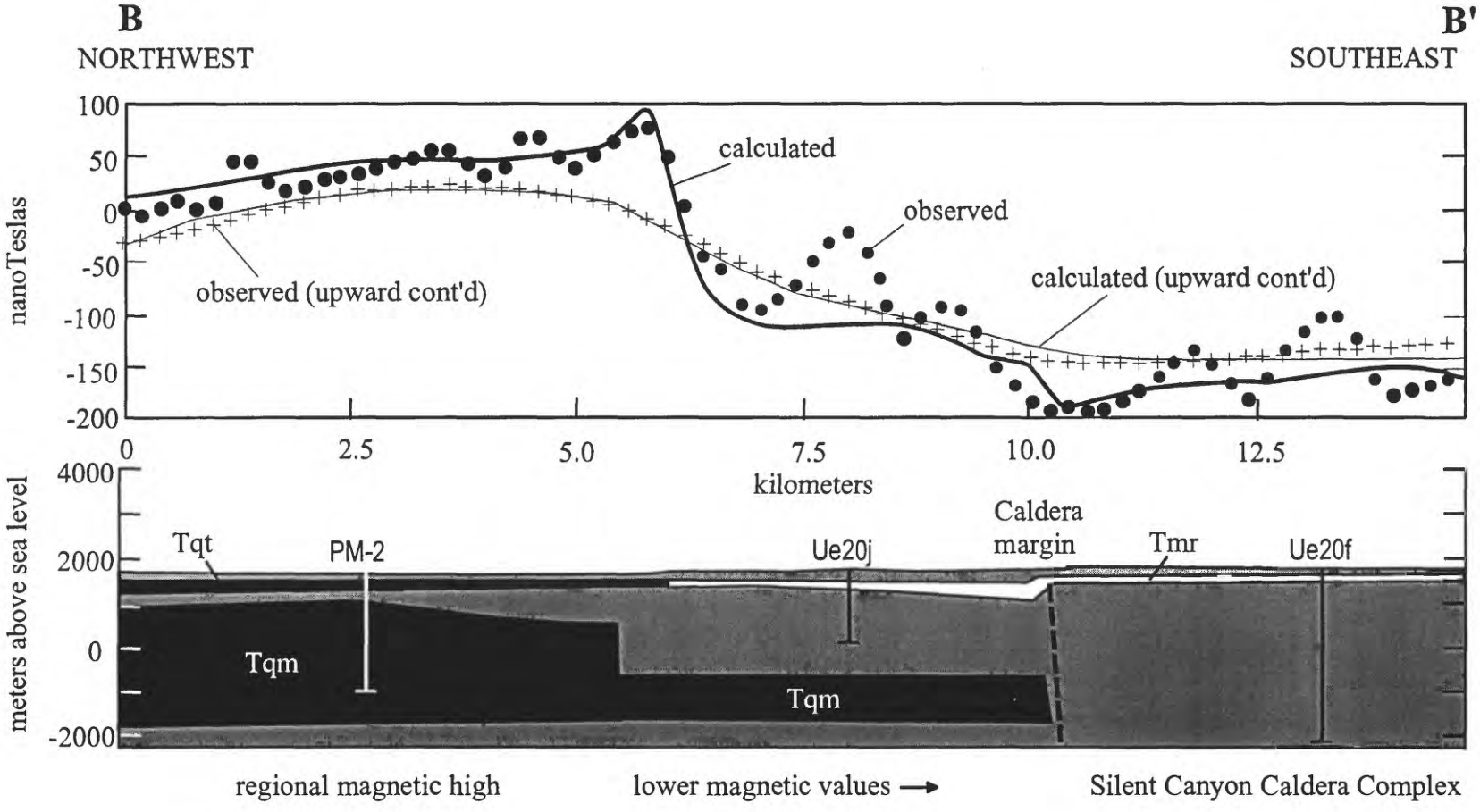

Figure 13 - Simple magnetic model for profile B-B' (located on figure 12b) northeast of Black Mountain, demonstrating the probable sources of the regional magnetic high. The magnetic field is calculated and observed at 122 m (bold line and dots) and 1122 m (thin line and plusses). Declination/inclination, and intensity (A/m) of total magnetization for tuff of Tolicha Peak (Tqt) = 24°/46°, 2.15; for Rainier Mesa Tuff (Tmr) = 157°/-32°, 1.08. The shallower body of dacite lava of Mt. Helen (Tqm) = 357°/58°, 0.9; the deeper body =15°/62°, 0.5. It is assumed that the deeper body has a lower remanent magnetization due to heating at depth (McElhinny, 1973). For simplicity, the gray area of the model has zero magnetization. Near the caldera margin, viable models require either thickening of the modeled Rainier Mesa Tuff, changes in magnetization, or variations in other rock units in this area. However, the chosen model shows the first possibility.

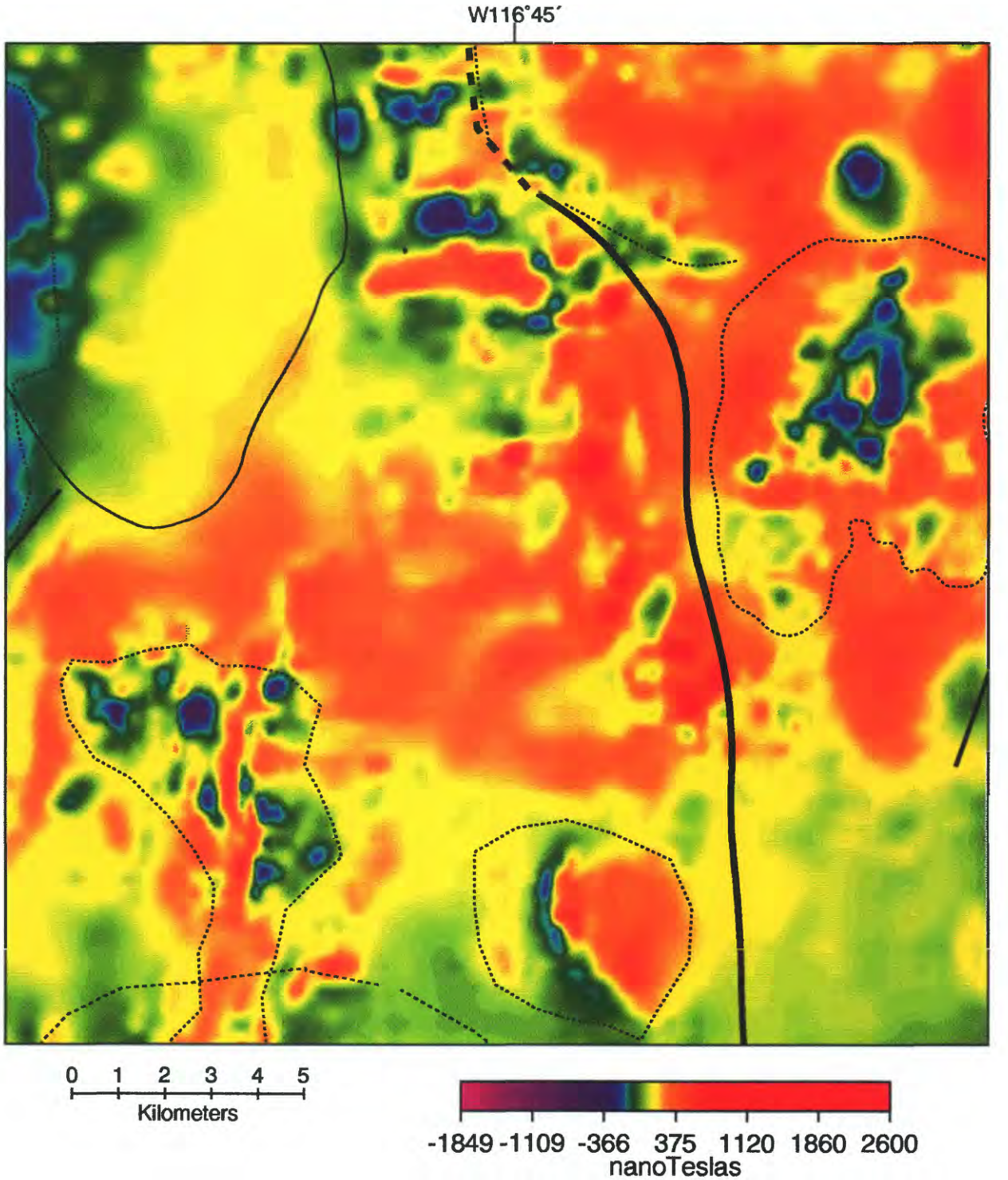

Figure 14b - Reduced-to-pole magnetic map for Thirsty Mountain (TM) and vicinity to the west, showing outlines of features from figure 6. Location of area shown on figure 6. Geologic overlay is figure 14a in pocket.

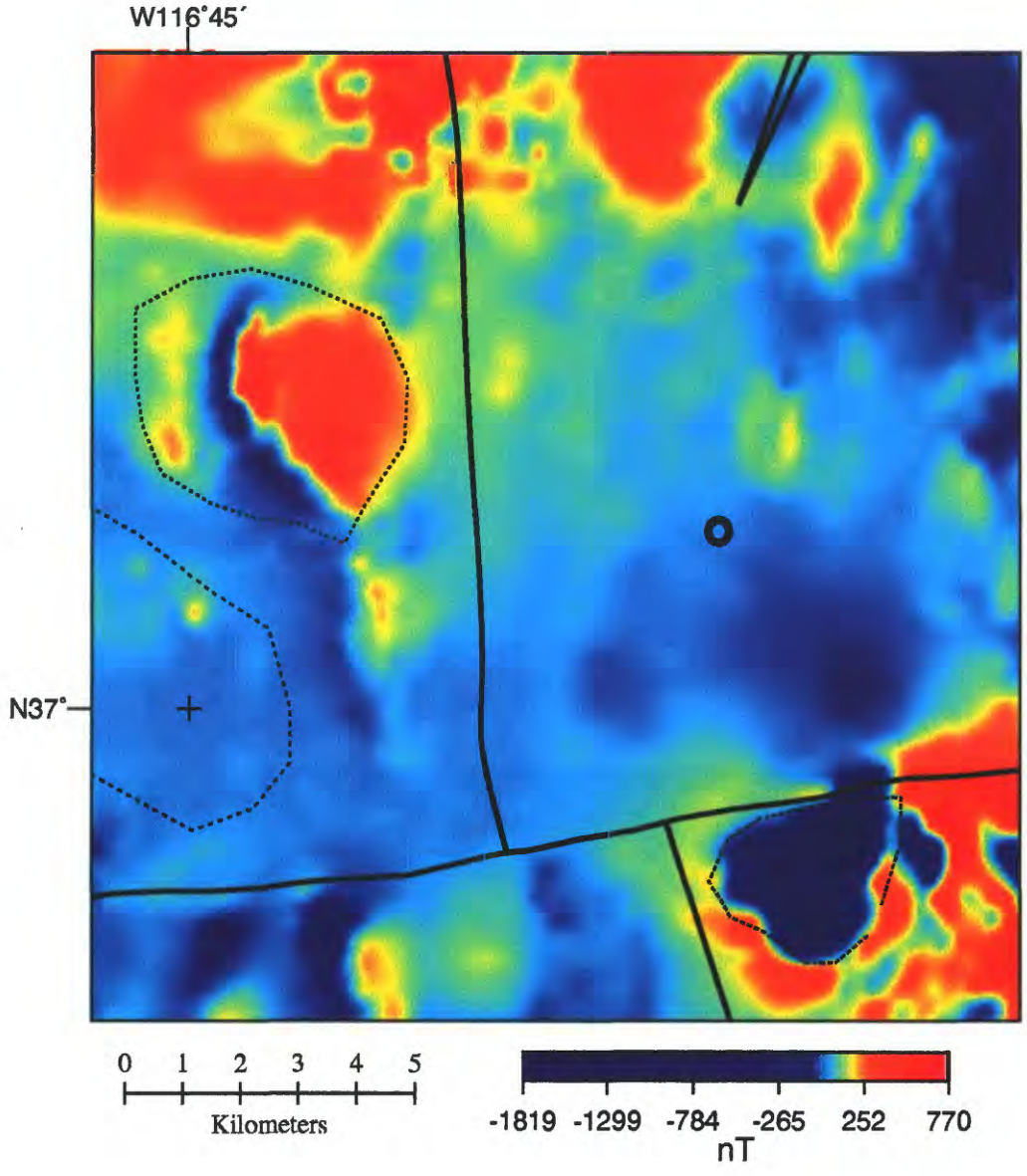

Figure 15b - Reduced-to-pole magnetic map for Oasis Valley basin with outlines of features from figure 6 and area of regional magnetic highs RHS and RHW of figure 7 (dot pattern). Note the change in color scale compared to other figures. Location of area shown on figure 6. Geologic overlay is figure 15a in pocket.

Table 1. Estimated reduction densities for investigating different lithologies in specified areas.

Reduction Density (kg/m^3)	Lithologies and Area	References
2000	Nonwelded tuff and alluvium, especially in Crater Flat and Yucca Mountain area	Snyder and Carr (1982; 1984); Ponce and Oliver (1995)
2200	Tuff and volcanic rocks for central caldera complexes, except for resurgent areas	Kane and others (1981); Healey (1968)
2400	Partially welded to welded tuff and other volcanic and intrusive rocks, especially associated with resurgent domes and around the outer margins of caldera complexes.	Kane and others (1981); Ponce and Oliver (1995); this study
2670	undivided pre-Tertiary sedimentary and igneous rocks surrounding SWNVF	Healey (1983); Ponce and Oliver (1995)
2750	pre-Tertiary carbonates and metamorphic rocks, especially in eastern NTS and in Bare Mountain and Funeral Mountains area	Langenheim (in press); Healey and others (1984)

TABLE 2. Selected volcanic units of the SWNVF and their descriptions and relative magnetic properties.

Caldera	Mag.[1] Signif.	Geologic Unit[2]	Approx. age (Ma)[3]	Description of Unit[3]	Maximum[3] Thickness (m)	Total magnetization[4]
	Quaternary Units					
		Qby Younger Quaternary basalt	0.35	Isolated cinder cones, lava flows, and feeder dikes on the flank of Sleeping Butte composed of trachybasalt and basalt		cinder cones: strong positive, elsewhere: weak[5]
	Younger Tertiary Units Tb					
	*	**Typ** Pliocene and youngest Miocene basalt at Thirsty Mountain	4.65	Basaltic trachyandesite erupted from shield volcano at Thirsty Mountain	>200	negative, strong[6]
	**	**Tyb** Thirsty Canyon and younger basalts	9.9-7.4	Widespread basalts spatially and temporally bracketing Thirsty Canyon Group peralkaline caldera volcanism	100	At Coba Ridge: negative, strong[6]; elsewhere: mixed polarities, strong[6]
	Thirsty Canyon Group Tt					
Black Mountain		**Ttg** Gold Flat Tuff	9.15	Strongly peralkaline, welded ashflow tuff		anomalous positive, weak[6]
	**	**Tth** Trachyte of Hidden Cliff	9.3	Sequence of very crystal-rich trachyte lavas emplaced as exogenous dome within a collapse depression in Black Mountain caldera	>500	positive, strong[6]
	Local *	**Tts** Trachytic rocks of Pillar Spring and Yellow Cleft	9.3	Trachyte to rhyolite lava flows, associated tuff and tuff breccia, and porphyritic syenite intrusive rocks; rocks partly fill and overlap Black Mountain caldera	180	negative, moderate[6]

TABLE 2 continued

Caldera Event	Mag.[1] Signif.	Geologic Unit[2]	Approx. Age (ma)[3]	Description of Unit[3]	Maximum[3] Thickness (m)	Total magnetization[4]
Black Mountain		**Ttt** Trail Ridge Tuff	9.3	Widespread welded, comendite ash-flow tuff	65	shallow negative, moderate[6]
	Local *	**Ttc** Comendite of Ribbon Cliff	9.4	Pre-caldera comendite and trachyte lava flows and domes exposed marginal to Black Mountain caldera	320	positive, strong[6]
	Volcanics of Fortymile Canyon Tf					
	*	**Tfu** Upper Fortymile rhyolite lavas in Bullfrog Hills	10.5-9.5	Rhyolite flows, domes, plugs, and associated tephra	175	negative, moderate[5]
	**	**Tfn** Trachyte of Donovan Mountain	10.4	Trachyte lava flows and subordinate feeder dikes, sills, and flow-margin tephra present in the Bullfrog Hills area.	>200	positive, strong[6]
	*	**Tfb** Beatty Wash Formation	11.4-11.2	Rhyolite lavas and related tuff erupted in moat of Timber Mountain caldera complex	lavas: 300-430; tuff: 60	positive, moderate[6] (only one site)
	Local *	**Tff** Rhyolite of Fleur-de-lis Ranch	11.4	Rhyolite lavas and welded ash-flow tuff erupted on west side of Timber Mountain caldera complex	300	positive, moderate[6]
	Timber Mountain Group Tm					
Ammonia Tanks	**	**Tma** Ammonia Tanks Tuff	11.45	Widespread metaluminous, welded ash-flow tuff; resurgently domed to form Timber Mountain.	intracaldera: >900; outflow: <150	positive, moderate-strong[6,7]
	**	**Tmat** Rhyolites of Tannenbaum Hill/Buried Canyon	11.55	Rhyolite lavas and related subordinate nonwelded tuff erupted in the moat of the Rainer Mesa caldera before collapse of the Ammonia Tanks caldera	>180	Tannenbaum Hill: positive, weak[6]; Buried Canyon: negative, strong[6]

TABLE 2 continued

Caldera Event	Mag.[1] Signif.	Geologic Unit[2]	Approx. Age (ma)[3]	Description of Unit[3]	Maximum[3] Thickness (m)	Total magnetization[4]
Rainier Mesa	**	**Tmr** Rainier Mesa Tuff	11.6	Voluminous and widespread, metaluminous, welded ash-flow tuff	intracaldera: >500; outflow: 150, locally ponded to 400	negative, moderate-strong,[6,7]
	Paintbrush Group Tp					
	*	**Tpu** Post-Tiva Canyon rhyolites	12.7	Post-caldera rhyolite lavas and related nonwelded tuff. Includes the rhyolite of Benham.	300	negative, strong[6]
Claim Canyon	**	**Tpc** Tiva Canyon Tuff	12.7	Widespread metaluminous welded ash-flow tuff. Locally hydrothermally altered in Bullfrog Hills	110	shallow negative, strong[8]
Unknown source	*	**Tpt** Topopah Spring Tuff	12.8	Widespread metaluminous welded ash-flow tuff	350	positive, moderate[8]
	Volcanics of Area 20					
		Tac Calico Hills Formation	12.9	Sequence of metaluminous rhyolite lavas and related tuff erupted from vents in the Calico Hills area and in the Area 20 caldera.	200, locally ponded to >2200.	Lavas: positive, moderate[6]; tuffs: positive, weak[6]
	Crater Flat Group Tc					
Area 20	*	**Tcb** Bullfrog Tuff	13.25	Widespread metaluminous, variably welded, rhyolite ash-flow tuff. Hydrothermally altered and locally brecciated in Bullfrog Hills	intracaldera: 680; outflow: 120	near Yucca Mt.: positive, strong[8] in Pahute Mesa: positive, weak-moderate[6]
Prospector Pass?	*	**Tct** Tram Tuff	13.4	Widespread welded rhyolite ash-flow tuff		negative, moderate[8]; strong at Tram Ridge[6]

TABLE 2 continued

Caldera Event	Mag.[1] Signif.	Geologic Unit[2]	Approx. Age (ma)[3]	Description of Unit[3]	Maximum[3] Thickness (m)	Total magnetization[4]
	Belted Range Group Tb					
		Tbd Deadhorse Flat Formation	13.7-13.5	Lavas and related tuff erupted and ponded within Grouse Creek Canyon caldera	1600	negative and mostly positive units, weak[6]
Grouse Canyon		**Tbg** Grouse Canyon Tuff	13.7	Peralkaline welded ash-flow tuff	intracaldera: 575; outflow: 110-150	shallow positive, weak[6]
	Volcanics of Quartz Mountain Tq					
Unknown source		**Tqs** Tuff of Sleeping Butte	14.3	Sequence of two metaluminous rhyolite ash-flow tuffs and associated bedded tephra	400	lower tuff: positive, strong[6]; other units: weak[5]
		Tqh Middle rhyolite of Quartz Mountain		Calc-alkaline rhyolite to dacite lava flows, small dome intrusions, and related tephra intercalated with compositionally similar bedded tuffs and local sedimentary rocks	lava flows: 250; bedded tuffs: 300	Lavas: negative, weak-moderate[6]
Unknown source	**	**Tqt** Tuff of Tolicha Peak	14.3	Metaluminous, welded rhyolite ash-flow tuff	300	positive, moderate-strong[6]
		Tqe Early rhyolite of Quartz Mountain		Calc-alkaline rhyolite to dacite lava flows and domes, commonly hydrothermally altered		unknown inclination, weak[5]
	OLDER VOLCANICS ON THE WEST					
	*	**Tqm** Dacite of Mount Helen		Lava flows and intrusive masses		positive, moderate[5] (see text)

TABLE 2 continued

Caldera Event	Mag.[1] Signif.	Geologic Unit[2]	Approx. Age (ma)[3]	Description of Unit[3]	Maximum[3] Thickness (m)	Total magnetization[4]
	OLDER VOLCANICS ON THE EAST					
	Volcanics of Big Dome					
Unknown source		**Tub** Tub Spring Tuff	14.9	Peralkaline welded ash-flow tuff	90	positive shallow, weak-moderate[6]
	Volcanics of Oak Spring Butte To					
Unknown source		**Toy** Tuff of Yucca Flat	15.05	Nonwelded to partly welded, metaluminous rhyolite ash-flow	80	negative shallow, weak-moderate[6]
Unknown source		**Tor** Redrock Valley Tuff	15.3	Welded, metaluminous, rhyolite ash-flow sheet	125	negative shallow, weak-moderate[6]
Unknown source		**Tot** Tuff of Twin Peaks	15.5	Rhyolite ash-flow tuff	475	negative, weak-moderate[6]

[1]Magnetically significant units are expected to produce magnetic anomalies. These are units that have (1) consistently moderate (*), or strong (**) total magnetization intensities (see note 4 below), (2) steep total magnetization inclinations or shallow inclinations (see note 4 below) with moderate to strong components aligned with or opposing the Earth's present-day field, (3) significant thickness and/or areal extent, and (4) clear correspondence to anomalies on the magnetic map. Some subjectivity was involved in this evaluation, especially regarding whether the measured magnetic properties were representative of the unit and whether the unit is volumetrically significant. The designation "Local" means that the unit is magnetically significant only in a very limited area.

[2]Unit names and groupings follow Sawyer and others (1995) and Warren and others (1989).

[3]From Sawyer and others (1995) and Fleck and others (1996).

[4]Total magnetizations are the vector sums of induced and remanent magnetization components. Inclinations are measured down from horizontal and are positive if > 25°; anomalous positive if < 25° and > 0°; negative if < -25°, and anomalous negative if > -25° but < 0°. Intensities are classified as suggested by Bath and Jahren (1984): nonmagnetic, < 0.05 A/m; weak, between 0.05 and 0.5 A/m; moderate, between 0.5 and 1.5 A/m; strong, >1.5 A/m.

[5]No total magnetization measurements available (although paleomagnetic properties only may have been reported); from inspection of magnetic map compared to geologic contacts and topography.

[6]From M. R. Hudson, unpub. data

[7]From Bath (1968)

[8]From Rosenbaum and Snyder (1985)

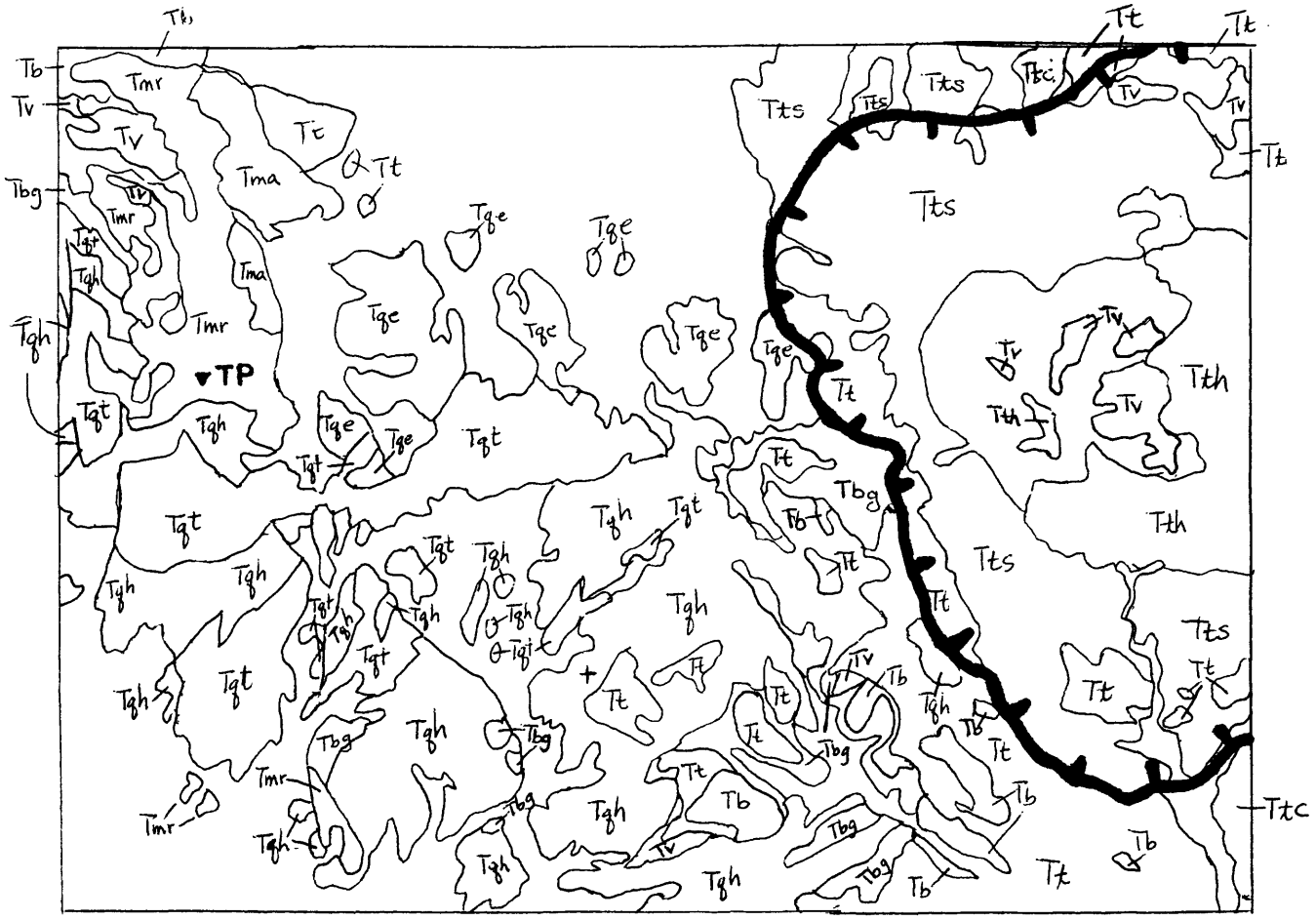

Figure 8a - Geologic overlay for Figure 8b. Map is generalized from Sawyer and others (1995). Units are described on Table 2, except for Tv, which refers to Tertiary volcanic units, undivided. TP, Tolicha Peak. Location of area shown on figure 6.

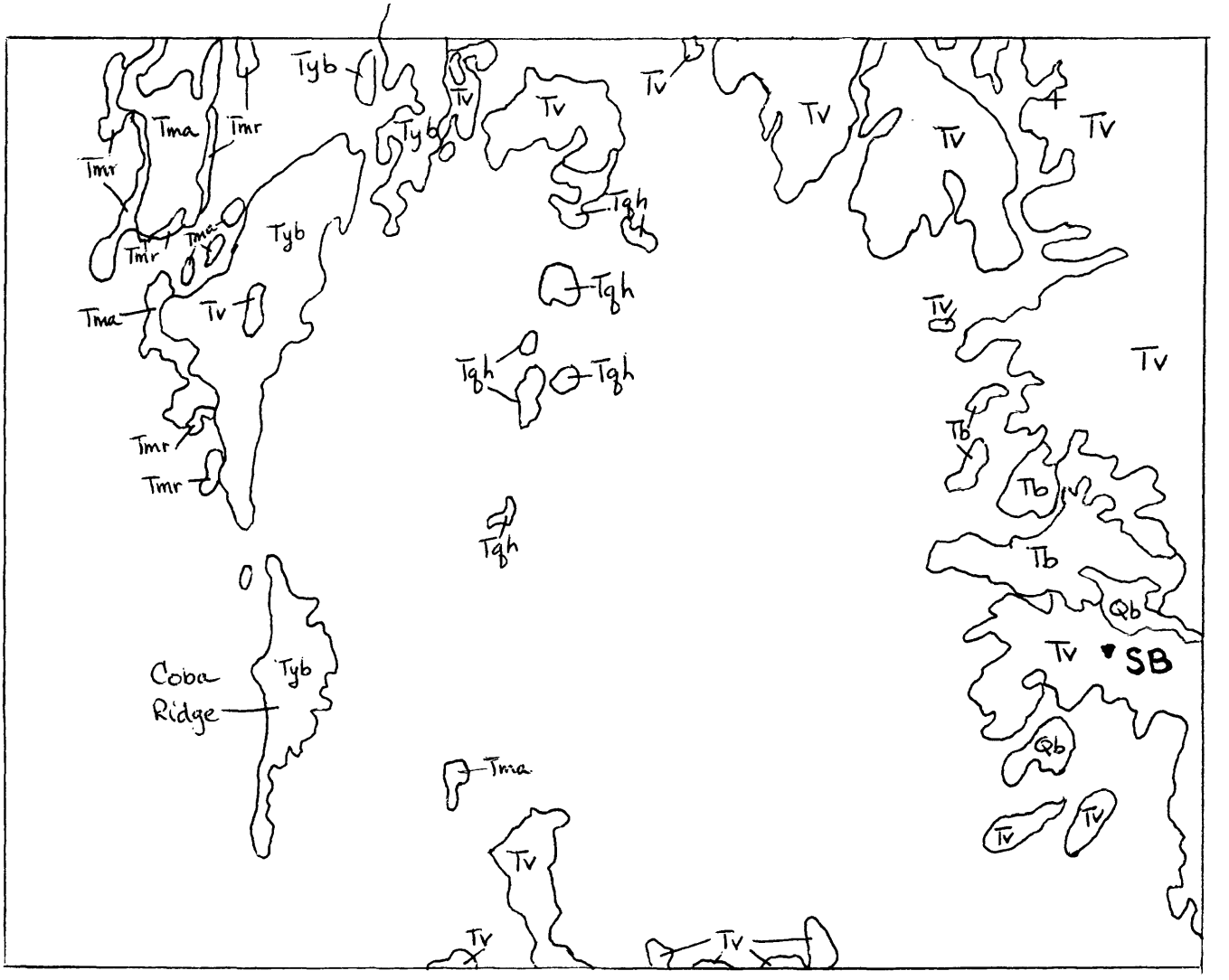

Figure 10a - Geologic overlay for Figure 10b. Map is generalized from Sawyer and others (1995). Units are described on Table 2, except for Tv, which refers to Tertiary volcanic units, undivided. SB, Sleeping Butte. Location of area shown on figure 6.

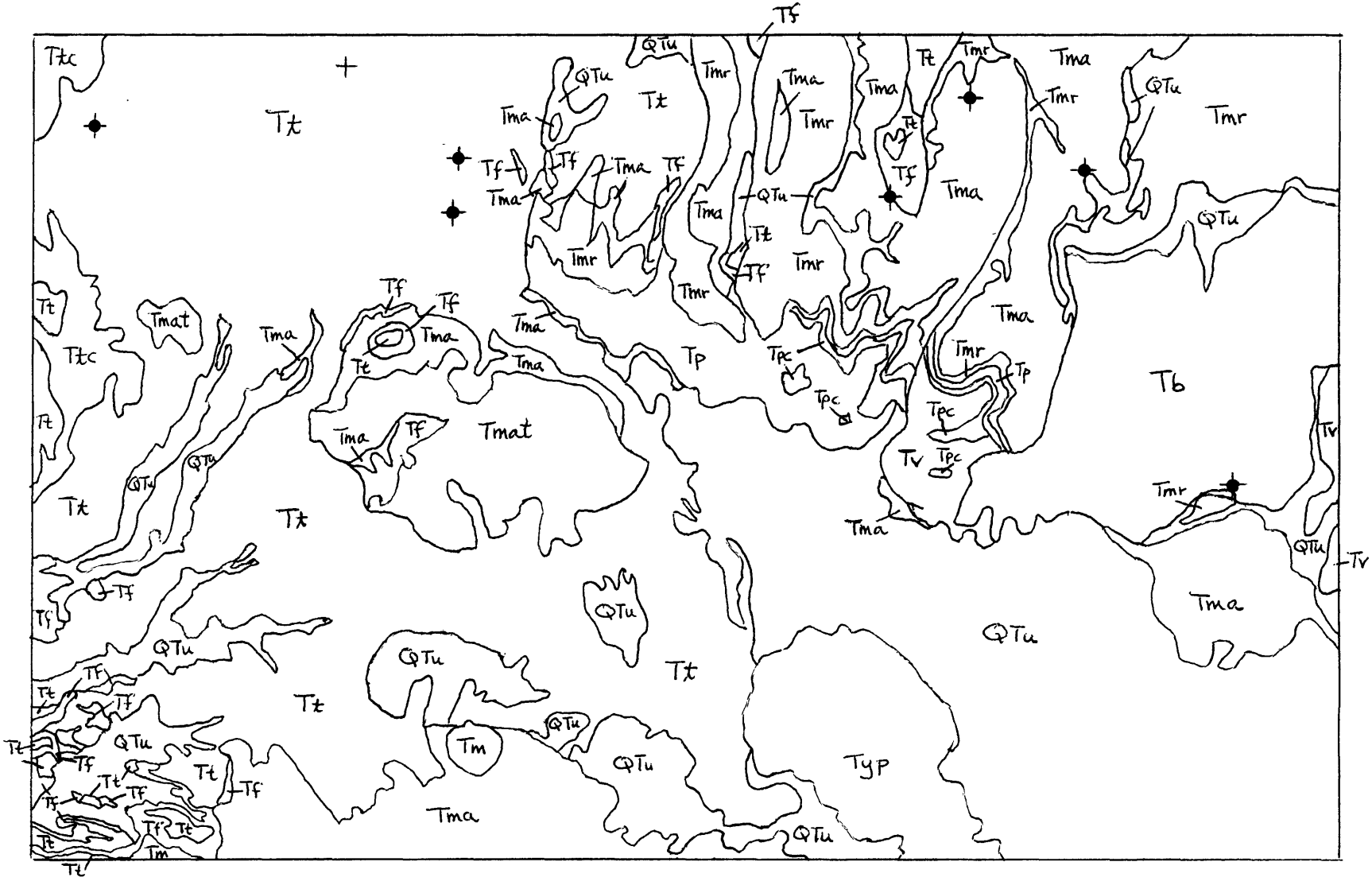

Figure 11a - Geologic overlay for Figure 11b. Map is generalized from Sawyer and others (1995). Units are described on Table 2, except for Tv, Tm, and Qtu, which refer to undivided Tertiary volcanic units, undivided Timber Mountain Group units, and undivided Quaternary and Tertiary sedimentary units, respectively. Drill holes discussed in text are shown by solid circles with plus.

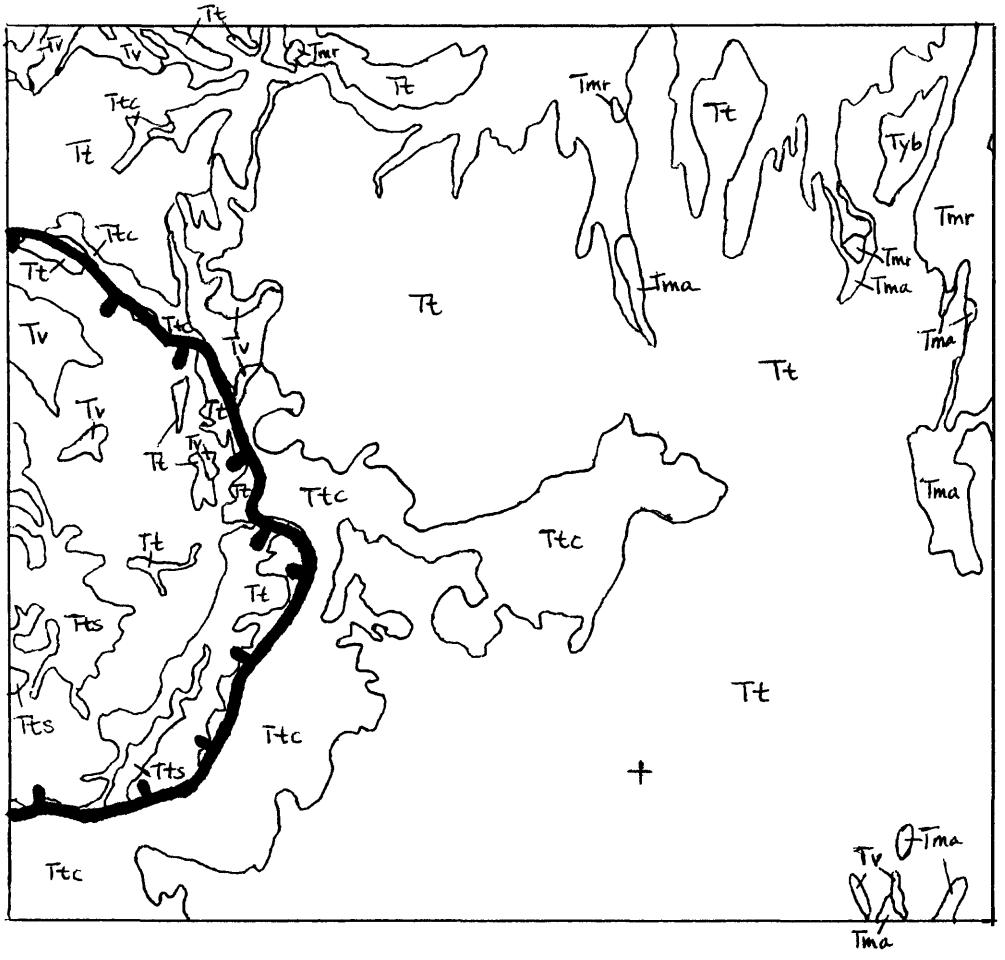

Figure 12a - Geologic overlay for Figure 12b. Map is generalized from Sawyer and others (1995). Units are described on Table 2, except for Tv, which refers to Tertiary volcanic units, undivided. Location of area shown on figure 6.

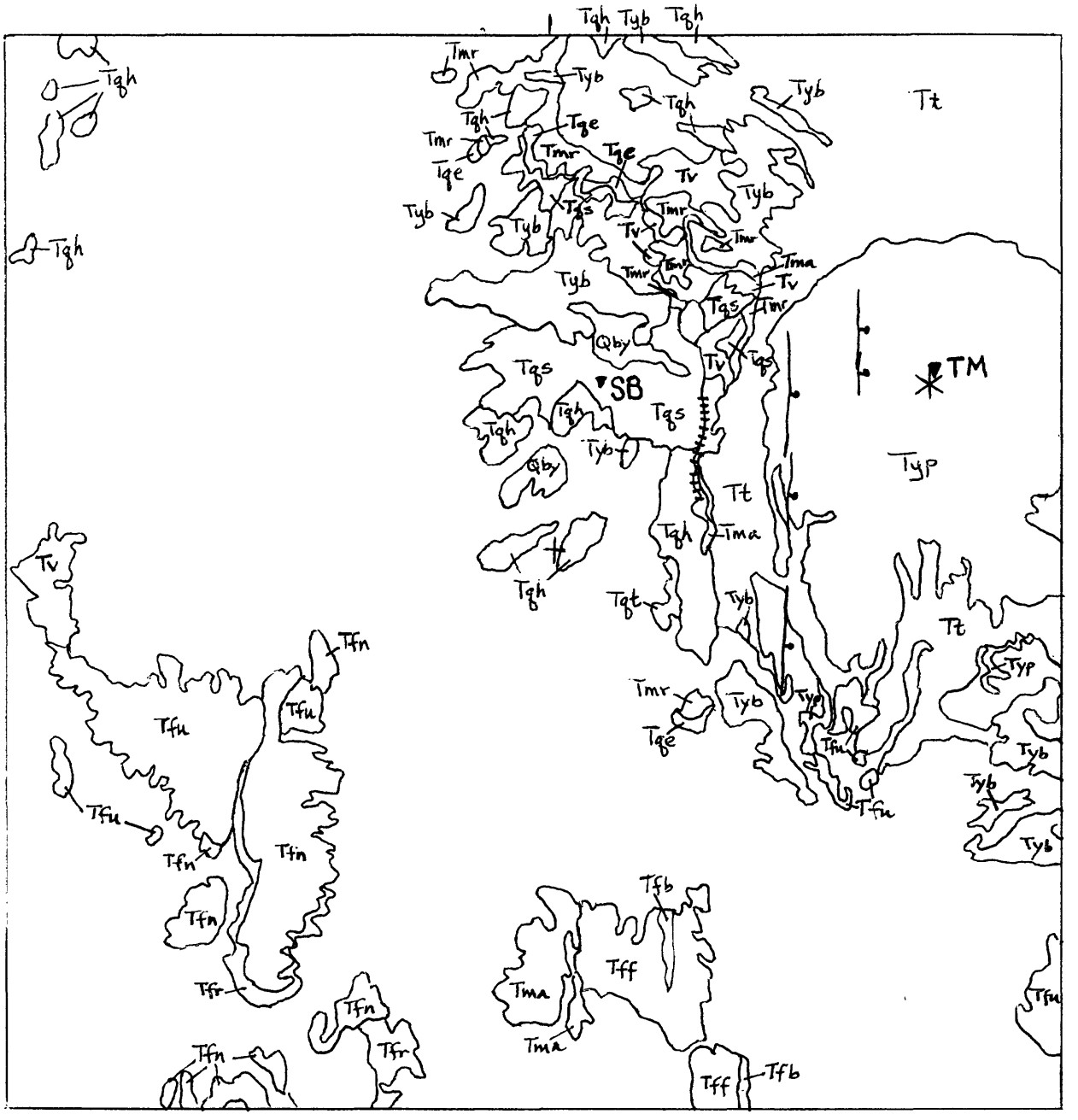

Figure 14a - Geologic overlay for Figure 14b. Map is generalized from Sawyer and others (1995). Units are described on Table 2, except for Tv, which refers to Tertiary volcanic units, undivided. Selected normal faults are shown west of Thirsty Mountain. A paleoscarp (Noble and others, 1991; Sawyer and others, 1995) is shown west of Thirsty Mountain by the railroad-track symbol. Location of area shown on figure 6.

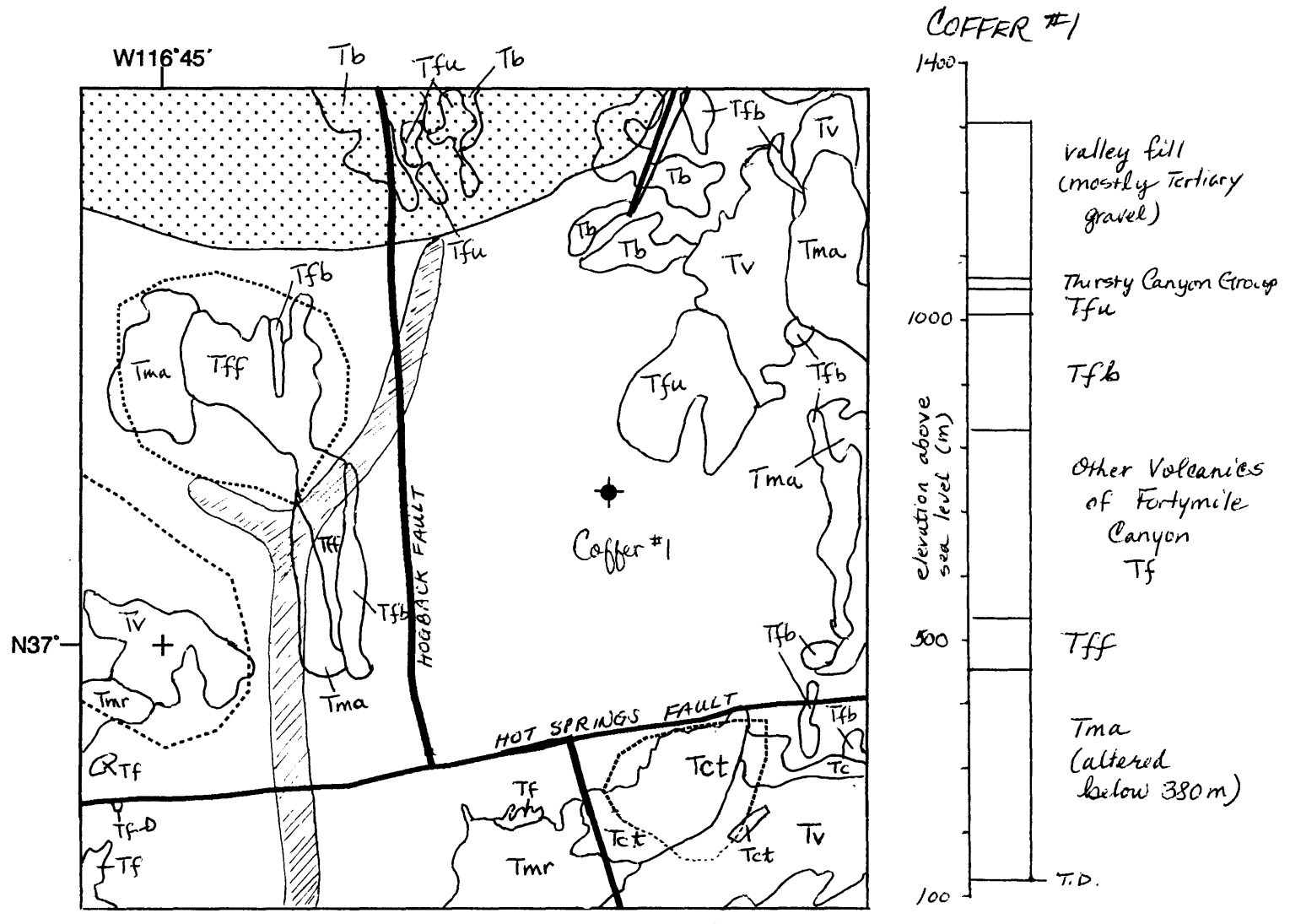

Figure 15a - Geologic overlay for Figure 15b and schematic stratigraphic section drilled in Coffer #1 well (R. Warren and D. Sawyer, written commun., 1992). Map is generalized from Sawyer and others (1995). Units are described on Table 2, except for Tv, which refers to Tertiary volcanic units, undivided. Oasis Valley discharge area is shown by the hachure pattern. Hogback and Hot Springs faults are informal names. Location of area shown on figure 6.